NASA/CR—2014–218444



Configuration and Evaluation of a Dual-Doppler 3-D Wind Field System

Winifred C. Crawford
ENSCO, Inc., Cocoa Beach, Florida
NASA Applied Meteorology Unit, Kennedy Space Center, Florida

November 2014

NASA STI Program ... in Profile

Since its founding, NASA has been dedicated to the advancement of aeronautics and space science. The NASA scientific and technical information (STI) program plays a key part in helping NASA maintain this important role.

The NASA STI program operates under the auspices of the Agency Chief Information Officer. It collects, organizes, provides for archiving, and disseminates NASA's STI. The NASA STI program provides access to the NTRS Registered and its public interface, the NASA Technical Reports Server, thus providing one of the largest collections of aeronautical and space science STI in the world. Results are published in both non-NASA channels and by NASA in the NASA STI Report Series, which includes the following report types:

- TECHNICAL PUBLICATION. Reports of completed research or a major significant phase of research that present the results of NASA Programs and include extensive data or theoretical analysis. Includes compilations of significant scientific and technical data and information deemed to be of continuing reference value. NASA counterpart of peer-reviewed formal professional papers but has less stringent limitations on manuscript length and extent of graphic presentations.

- TECHNICAL MEMORANDUM. Scientific and technical findings that are preliminary or of specialized interest, e.g., quick release reports, working papers, and bibliographies that contain minimal annotation. Does not contain extensive analysis.

- CONTRACTOR REPORT. Scientific and technical findings by NASA-sponsored contractors and grantees.

- CONFERENCE PUBLICATION. Collected papers from scientific and technical conferences, symposia, seminars, or other meetings sponsored or co-sponsored by NASA.

- SPECIAL PUBLICATION. Scientific, technical, or historical information from NASA programs, projects, and missions, often concerned with subjects having substantial public interest.

- TECHNICAL TRANSLATION. English-language translations of foreign scientific and technical material pertinent to NASA's mission.

Specialized services also include organizing and publishing research results, distributing specialized research announcements and feeds, providing information desk and personal search support, and enabling data exchange services.

For more information about the NASA STI program, see the following:

- Access the NASA STI program home page at http://www.sti.nasa.gov

- E-mail your question to help@sti.nasa.gov

- Phone the NASA STI Information Desk at 757-864-9658

- Write to:
  NASA STI Information Desk
  Mail Stop 148
  NASA Langley Research Center
  Hampton, VA 23681-2199

NASA/CR—2014–218444



Configuration and Evaluation of a Dual-Doppler 3-D Wind Field System

Winifred C. Crawford
ENSCO, Inc., Cocoa Beach, Florida
NASA Applied Meteorology Unit, Kennedy Space Center, Florida

National Aeronautics and
Space Administration

Kennedy Space Center
Kennedy Space Center, FL 32899-0001

November 2014

Acknowledgments

The author thanks Ms. Jackie Shafer and Dr. William Bauman of the AMU and Mr. Erik Magnuson of ENSCO, Inc. for their assistance in setting up the Linux PC and assisting with Linux training; WDSS II developers and experts Dr. Valliappa Lakshmanan, Benjamin Herzog, and Jeff Brogden for their assistance in determining the appropriate tools and tool options to use in WDSS-II; Mr. Pete Blottman for supplying the TDWR data, Mr. Todd McNamara for supplying the WSR data, and Mr. Fritz O'Hora for his knowledge of working with the WSR data.

Available from:

NASA Center for AeroSpace Information
7115 Standard Drive
Hanover, MD 21076-1320
443-757-5802

This report is also available in electronic form at

http://science.ksc.nasa.gov/amu

Executive Summary

Customer: NASA's Launch Services Program (LSP), Ground Systems Development and Operations (GSDO), and Space Launch System (SLS) programs; and the National Weather Service in Melbourne, Florida (NWS MLB).

Current LSP, GSDO, and SLS space vehicle operations are halted when wind speeds from specific directions exceed defined thresholds and when lightning is a threat. Strong winds and lightning are difficult parameters for the 45th Weather Squadron (45 WS) to forecast, yet are important in the protection of customer vehicle operations and the personnel that conduct them. A display of the low-level horizontal wind field to reveal areas of high winds or convergence would be a valuable tool for forecasters in assessing the timing of high winds, or convection initiation and subsequent lightning occurrence. This is especially important for areas where no weather observation platforms exist. Developing a dual-Doppler radar capability would provide such a display to assist forecasters in predicting high winds and convection initiation. The wind fields can also be used to initialize a local mesoscale numerical weather prediction model to help improve the model forecast winds, convection initiation, and other phenomena.

The 45 WS and NWS MLB tasked the Applied Meteorology Unit (AMU) to develop a dual-Doppler wind field display using data from the 45th Space Wing radar, known as the Weather Surveillance Radar (WSR), NWS MLB Weather Surveillance Radar 1988 Doppler (KMLB), and the Orlando International Airport Terminal Doppler Weather Radar (KMCO). They also stipulated that the software used should be freely available. The AMU evaluated two software packages and, with concurrence from NWS MLB and the 45 WS, chose the Warning Decision Support System-Integrated Information (WDSS-II).

The AMU collected data from two significant weather cases: a tornadic event on 14 April 2013 and a severe wind and hail event on 12 February 2014. For the 14 April case, the data were from WSR and KMLB. For the 12 February case, the data were from KMCO and KMLB. The AMU installed WDSS-II on a Linux PC, then processed and quality controlled the radar data for display and analysis using WDSS-II tools. Because of issues with de-aliasing the WSR velocity field, the AMU did not use data from this radar in this study and only analyzed the 12 February case.

Merging the data to create the dual-Doppler analysis involved several steps. The AMU used instructions from the WDSS-II website and discussion forum to determine the correct tools to use for the analysis, and was successful in creating a merged reflectivity field, which was critical to the success of creating a merged velocity field. However, the AMU was unable to create a merged velocity field. The AMU researched the WDSS-II forum for discussions on similar issues, asked questions on the forum, and tested different options and values in the merger tool with no success.

Developing a dual-Doppler wind field was the main goal of this task, but that was not accomplished. It could be an issue of not using the correct options or the correct value for the options used, or there could be issues with the radar data. There is a follow-on AMU task to install the operational version of WDSS-II in the NWS MLB office. This will provide more opportunities to try different options and input values in order to create a merged wind field from KMCO and KMLB.

Table of Contents

Executive Summary 3

Table of Contents 4

List of Figures 6

List of Tables 8

1 Introduction 9

1.1 Previous Work 9

1.2 Current Work 9

2 Radar Data and Analysis Tools 10

2.1 Radar Data 10

2.1.1 WSR-88D 10

2.1.2 WSR 11

2.1.3 TDWR 11

2.2 Analysis Tools: Software and Hardware 13

2.2.1 Software 13

2.2.2 Hardware 13

3 WDSS-II Preparation 14

3.1 WDSS-II Setup 14

3.2 WDSS-II Data Processing 15

3.2.1 Reflectivity Data QC 15

3.2.2 Velocity Data De-aliasing 15

3.2.2.1 KMLB 16

3.2.2.2 WSR 18

3.3 WDSS-II Display 20

4 Data Merger in WDSS-II 24

4.1 Merger Grid 24

4.2 Reflectivity Merger 25

4.3 Velocity Merger 27

5 Conclusions 30

5.1 Summary 30
5.2 Using WDSS-II 30
5.3 Recommended Future Work 31
Appendix: WDSS-II Setup and Use Details 32
References 49
List of Acronyms 50

List of Figures

Figure 1. Google Earth image showing the locations of the MCO TDWR, 45 SW WSR, and NWS MLB WSR-88D. 10

Figure 2. The form on the WDSS-II website used to get access to the software package. 14

Figure 3. KMLB 8.0° velocity at 0040 UTC on 15 April 2013, a) aliased velocity and b) de-aliased velocity. The locations of the WSR-88D and 45 SW WSR radars are shown by the yellow circles, and the circle and ellipse highlight locations of the aliased (a) and de-aliased (b) velocities. 17

Figure 4. WSR 10.9° velocity at 0040 UTC on 15 April 2013, a) aliased velocity and b) de-aliased velocity. The locations of the WSR-88D and 45 SW WSR radars are shown by the yellow circles, and the circles highlight locations of aliased (a) and de-aliased (b) velocities. 19

Figure 5. The initial screen in WDSS-II when issuing the wg command in a terminal window. The processes used to load data are highlighted by red rectangles with red arrows showing the sequence to get the dialog box that allows the user to browse for the data directory. 21

Figure 6. The WDSS-II GUI with data and map background displayed. The Sources section contains a tab named “Feb12-KMCO” with the choices of radar product (left column), elevation angle (middle column), and scan time (right column) for KMCO on 12 February 2014. The highlighted items in each list determine what is displayed: the 0.3° QC’d reflectivity at 213527 UTC. 22

Figure 7. Same data as Figure 6, but showing the Products tab containing a list of the data sets that have been loaded for display and the controls for changing elevation angles and times. 23

Figure 8. Google Earth image of the dual-Doppler lobes and associated merger grid outline for KMCO and KMLB. 25

Figure 9. The KMCO reflectivity at 2316 UTC 12 February 2014, elevation angle 0.3 degrees. The yellow circles show the locations of the KMCO and KMLB radars. 26

Figure 10. As in Figure 9 but for KMLB reflectivity at 2318 UTC, elevation angle 0.5 degrees. 26

Figure 11. The KMCO and KMLB merged reflectivity at 2316 UTC 12 February 2014, height of 1 km. 27

Figure 12. The KMCO velocity at 2212 UTC 12 February 2014, elevation angle 1.0 degrees. The yellow circles show the locations of the KMCO and KMLB radars. 28

Figure 13. As in Figure 12, but for the KMLB velocity at 2211 UTC, elevation angle 1.3 degrees. 28

Figure 14. The KMCO and KMLB merged velocity at 2211 UTC 12 February 2014, height of 3 km. 29

Figure 15. The top portion of the WDSS-II home page. The links with information on how to install and use WDSS-II are in the left column under the Documentation link. 31

List of Appendix Figures

Figure 1. Content of the .bashrc file. 32

Figure 2. The new dialog box displayed after clicking the Browse… button on the initial dialog box (section 3.3, Figure 5). The chosen directory is surrounded by the red box, the desired code_index.xml file is highlighted in blue on the right side. 37

Figure 3. The initial dialog box (section 3.3, Figure 5) showing the chosen input file in the URL text box and the user-supplied name in the Name text box. 38

Figure 4. The WDSS-II display showing KMCO data on 12 February 2014 at 213527 UTC. The Sources section displays the loaded radar data parameters to choose for display. The left column contains the radar products, the middle column contains the elevation angles, and the right column contains the time of each scan. 39

Figure 5. WDSS-II with the map background that comes with the software. The data are the same as in Figure 4, but zoomed out. 40

Figure 6. Contents of the maps.xml file in the w2config/maps directory. 41

Figure 7. The Add New Map dialog box is displayed after clicking on Add… in the Maps menu. The State map is highlighted. 41

Figure 8. The WDSS-II GUI displaying the state and county boundaries using the same data and zoom level as Figure 6. The Earth map is highlighted to show how to eliminate a map background without deleting it from the list by checking the box next to Hide in the Maps section. 42

Figure 9. Similar to Figure 6 in section 3.3, except the Sources tab contains a second tab named “Feb12-KMLB”. The highlighted items in each list determine what is displayed: the KMLB 0.5° QC’d reflectivity at 213307 UTC. 43

Figure 10. Similar to Figure 9, except for the de-aliased velocity at 213324 UTC and showing the Products tab contents. The buttons with a red box control the time displayed and the buttons with a green box control the elevation angle displayed. ..44

List of Tables

Table 1. The VCPs used for the NWS MLB WSR-88D, 45 SW WSR, and the MCO TDWR during the 14 April 2013 and 12 February 2014 case study time periods. For the WSR, the Default VCP was used on 14 April. The 45 SW VCP is included for completeness. 12

1 Introduction

Current Launch Services Program, Ground Systems Development and Operations, and Space Launch System space vehicle operations are halted when wind speeds from specific directions exceed defined thresholds and when lightning is a threat. Strong winds and lightning are difficult parameters for the 45th Weather Squadron (45 WS) to forecast, yet are important in the protection of customer vehicle operations and the personnel that conduct them. A display of the low-level horizontal wind field to reveal areas of high winds or convergence would be a valuable tool for forecasters in assessing the timing of high winds impacting operations, or convection initiation and subsequent lightning occurrence. This is especially important for areas where no weather observation platforms exist. Developing a dual-Doppler weather radar capability would provide such a display to assist forecasters in predicting high winds and convection initiation. The wind fields can also be used to initialize a local mesoscale numerical weather prediction model to help improve the model forecast winds, convection initiation, and other phenomena. Finally, data combined from multiple radars would lessen radar geometry problems such as the cone of silence and beam blockage. This display would aid in using ground processing and space launch resources more efficiently by stopping or starting work in a timelier manner.

1.1 Previous Work

A previous Applied Meteorology Unit (AMU) task (Huddleston 2012) investigated the technical, hardware, and software requirements necessary to create a dual-Doppler capability using the 45 Space Wing (45 SW) Radtec 43/250 and the National Weather Service in Melbourne, Florida (NWS MLB) Weather Surveillance Radar 1988-Doppler (WSR-88D) radars. The evaluation showed that the creation of a dual-Doppler capability using the existing operational radar systems was feasible. However, data security and cost considerations had to be taken into consideration in light of current budgetary constraints.

NWS MLB also expressed interest in this task, and suggested including data from the Federal Aviation Administration Terminal Doppler Weather Radar (TDWR) at Orlando International Airport (MCO). In addition, in the event of a radar outage at one of the sites, the multi-radar algorithms would provide continuing coverage of the area through use of the data from the remaining operational radar sites.

1.2 Current Work

With the positive results in Huddleston (2012), the 45 WS and NWS MLB tasked the AMU to develop a dual-Doppler wind field display using data from the 45 SW radar, known as the Weather Surveillance Radar (WSR), NWS MLB WSR-88D (KMLB), and the MCO TDWR (KMCO). They also stipulated that the software used to derive the wind field over east-central Florida should be freely available. The AMU evaluated two software packages and, with concurrence from NWS MLB and the 45 WS, chose the Warning Decision Support System-Integrated Information (WDSS-II; www.cimms.ou.edu/~lakshman/WDSS2/index.shtml).

2 Radar Data and Analysis Tools

The AMU collected data from the three local Doppler radars identified in section 1.2. The tools needed for the analysis included software and a computer with sufficient computing power and memory to run the software and store the input and output data.

2.1 Radar Data

As stated previously, data from three local Doppler radars were used in this task: KMLB, WSR located west of the Kennedy Space Center (KSC)/Cape Canaveral Air Force Station (CCAFS) area, and KMCO. Figure 1 shows the radar locations.

Data from two significant weather events were collected for the analysis: 14 April 2013 and 12 February 2014. During the evening of 14 April, two F-0 tornados, winds in excess of 50 kt, and 1-inch hail occurred in and surrounding Brevard County, Florida, which is in NWS MLB's county warning area (CWA) and contains KSC/CCAFS. On 12 February, winds in excess of 50 kt and quarter-size hail were reported in some central Florida locations beyond Brevard County, but near and within the CWA.

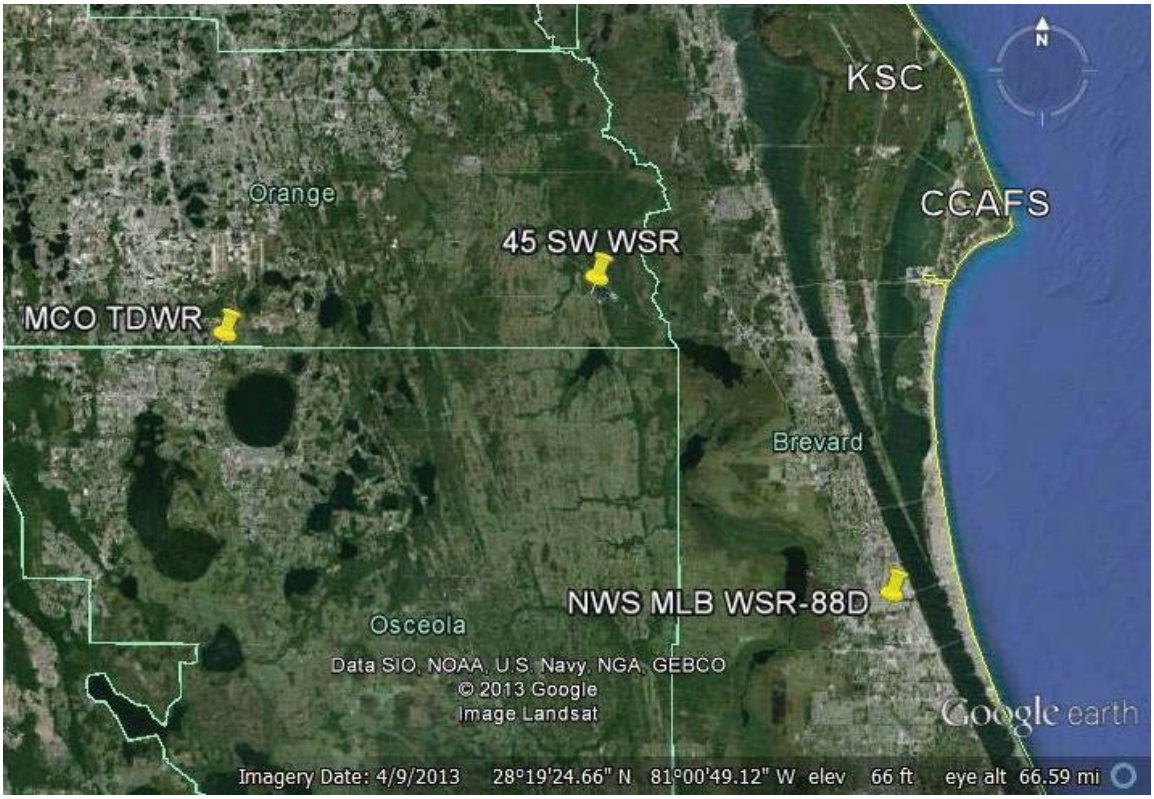


Figure 1. Google Earth image showing the locations of the MCO TDWR, 45 SW WSR, and NWS MLB WSR-88D.

2.1.1 WSR-88D

KMLB is a Doppler radar with dual-polarization technology. It is an S-band radar with a 10-cm wavelength. The beam width is 1° and gate spacing along the beam is 0.25 km. The WSR-88D uses several volume coverage patterns (VCPs), which are sets of elevation angles the radar goes through in a specific sequence. The choice of VCP depends on the weather conditions and is controlled by the operator.

Data for both severe weather events described in section 2.1 were downloaded from the National Climatic Data Center (NCDC). The files were in Level II format, which contain the base data values for reflectivity, mean radial velocity, and spectrum width, and the dual-pol data values for differential reflectivity, correlation coefficient, and differential phase. Each file contains a complete volume scan with data from all elevation angles in the VCP. On the days used in this task, KMLB was predominantly in VCP 12, which has 14 elevation angles and was designed for use during severe convective events. The angles associated with VCP 12 and the order in which they are scanned are shown in Table 1. The first three angles are scanned twice, first for reflectivity and then for velocity. It took approximately 4 min 40 sec to scan through the elevation angles in VCP 12. Level-II format files can be processed by WDSS-II routines.

2.1.2 WSR

The 45 SW WSR is also a Doppler radar with dual-polarization technology. It is a C-band radar with a 5.3-cm wavelength. The beam width is 0.95° and gate spacing along the beam is 0.25 km. The 45 SW VCP is based on recommendations from the AMU (Short 2008) and meets a 45 SW requirement for minimizing the vertical gaps between beams. It has 13 elevation angles that scan in an interleaving pattern, going through every other angle on the way up and down. It takes approximately 2 min 50 sec to scan through the elevation angles in the 45 SW VCP. This scan strategy provides the 45 WS forecasters with improved monitoring of

- low-level convergence in the boundary layer that contributes to thunderstorm development;
- the atmospheric electrification layer (+5 C to -20 C) for evaluating lightning launch commit criteria (LLCC) and predicting lightning onset;
- the layer where convective cloud tops and anvil clouds typically occur (25-40,000 ft) for evaluating LLCC; and
- thunderstorms approaching from the southwest due to the reduced cone of silence (Roeder and Short 2009).

Data from the 14 April case were collected from this radar. The files were provided by Mr. McNamara of the 45 WS. WSR data are in Vaisala's Sigmet Interactive Radar Information System (IRIS™) format, and the files contain the same base and dual-pol values as the WSR-88D Level II data. Each file contains data from one elevation angle. The VCP used during the 14 April event was the system default. As a result of an ongoing software upgrade project, the VCP sometimes changed to the default setting when the system was changed to a baseline configuration. The forecasters and LWOs were sometimes unaware of this change unless they noticed something different on the display. Once noticed, they would make the change back to the 45 SW VCP. Maintenance and a baseline change had recently been done on the WSR in April 2013, causing the system default VCP to be used for this case. This will not be an issue once the software upgrade project is complete. Table 1 shows the elevation angles in the 45 SW VCP and the elevation angles in the default VCP used in this data set in the order they are scanned. The IRIS files can be processed by WDSS-II algorithms.

2.1.3 TDWR

KMCO is a Doppler radar but does not have dual-polarization capability. Like the WSR, it is a C-band radar with a 5.3-cm wavelength. The beam width is 0.55° and gate spacing along the beam is 0.15 km. TDWR has two VCPs: VCP 90, called Monitor mode, and VCP 80, called Hazardous mode. The specific elevation angles for each VCP vary among TDWR sites, and are dependent on the range of the radar from the airport. Table 1 shows the angles in both VCPs for MCO. The VCP in use is chosen automatically by the TDWR software based on echo intensity,

coverage, and range to the airport. It takes approximately six minutes to scan through the elevation angles in both VCPs. In VCP 90, the elevation angles are scanned sequentially from lowest to highest in a volume scan. In VCP 80, the lowest angle is scanned every minute and the upper angles are scanned in two sequences.

Files for the 14 April case were sent to the AMU by Mr. Paul Biron of the FAA, but WDSS-II could not process the file format. WDSS-II does have algorithms that can process the files taken directly from the Supplemental Product Generator (SPG). TDWR data are archived on the SPG for eight days and then overwritten. Work on this task started well after the 14 April case, meaning files for that day were no longer available on the NWS MLB SPG. Therefore, data from the other severe weather case on 12 February were collected from the SPG located in the NWS MLB office by Mr. Blottman of NWS MLB. The MCO TDWR primarily used VCP 80 on 12 February.

Table 1. The VCPs used for KMLB, WSR, and KMCO during the 14 April 2013 and 12 February 2014 case study time periods. For the WSR, the Default VCP was used on 14 April. The 45 SW VCP is included for completeness.

KMLB	*WSR*		*KMCO*	
VCP 12	*Default*	*45 SW*	*VCP 90*	*VCP 80*
0.5	0.2	0.2	0.3	0.3
0.5	0.4	2.2	0.3	0.3
0.9	3.2	5.7	1.0	1.0
0.9	6.6	8.9	3.3	3.3
1.3	10.9	12.5	6.1	6.6
1.3	16.1	17.6	11.0	0.3
1.8	22.4	28.3	15.9	10.0
2.4	26.0	22.0	20.8	13.4
3.1	19.1	14.5	25.7	16.8
4.0	13.4	10.6	30.6	0.3
5.1	8.6	7.3	35.5	29.9
6.4	4.8	4.0	40.4	60.0
8.0	1.8	1.2	45.3	3.3
10.0			50.2	0.3
12.5			55.1	6.6
15.6			60.0	10.0
19.5				13.4
				0.3
				16.8
				29.9
				60.0
				0.3

2.2 Analysis Tools: Software and Hardware

The AMU considered two free software packages to conduct the analysis and determined the computing resources needed for each.

2.2.1 Software

Huddleston (2012) identified three software packages that can be used to create a dual-Doppler analysis: a set of programs from The National Center for Atmospheric Research (NCAR), WDSS-II, and an add-on product for the 45 SW's IRIS software called NDOP. Vaisala's cost for NDOP at the time of that study was $16,000. Since the AMU was tasked to find freely available software because the 45 SW and KSC Weather Office budgets did not allow for software purchase, NDOP was not considered for this task. However, it should remain a consideration should funds become available in the future.

The NCAR radar processing programs can, among other capabilities, create dual- and multi-Doppler analyses (https://wiki.ucar.edu/display/raygridding/Home). This software was used in Dolan and Rutledge (2007) to create multi-Doppler analyses in real time. It is also used by researchers at the University of Alabama in Huntsville (Dr. Lawrence Carey, personal communication). Mr. Jay Miller, retired from NCAR, is the contact point for the software and stated that he is working on updating the software and creating tutorials. That update is ongoing.

The WDSS-II package was developed jointly by the Cooperative Institute for Mesoscale Meteorological Studies (CIMMS) at the University of Oklahoma (OU) and the National Severe Storms Laboratory. It has several capabilities including routines to merge Doppler radar velocity data onto a grid. The version available for free download can only be used in research mode. A license is needed for the operational version, but the licensed version is free for the NWS. (www.cimms.ou.edu/~lakshman/WDSS2/index.shtml).

After considering the positives and negatives of each software package and consulting with NWS MLB, the AMU chose the research version of WDSS-II to conduct the analysis. The ongoing updates to the NCAR software and the multiple programs involved could make it difficult to work with. WDSS-II has other capabilities besides merging radar data and is in use at several NWS offices.

2.2.2 Hardware

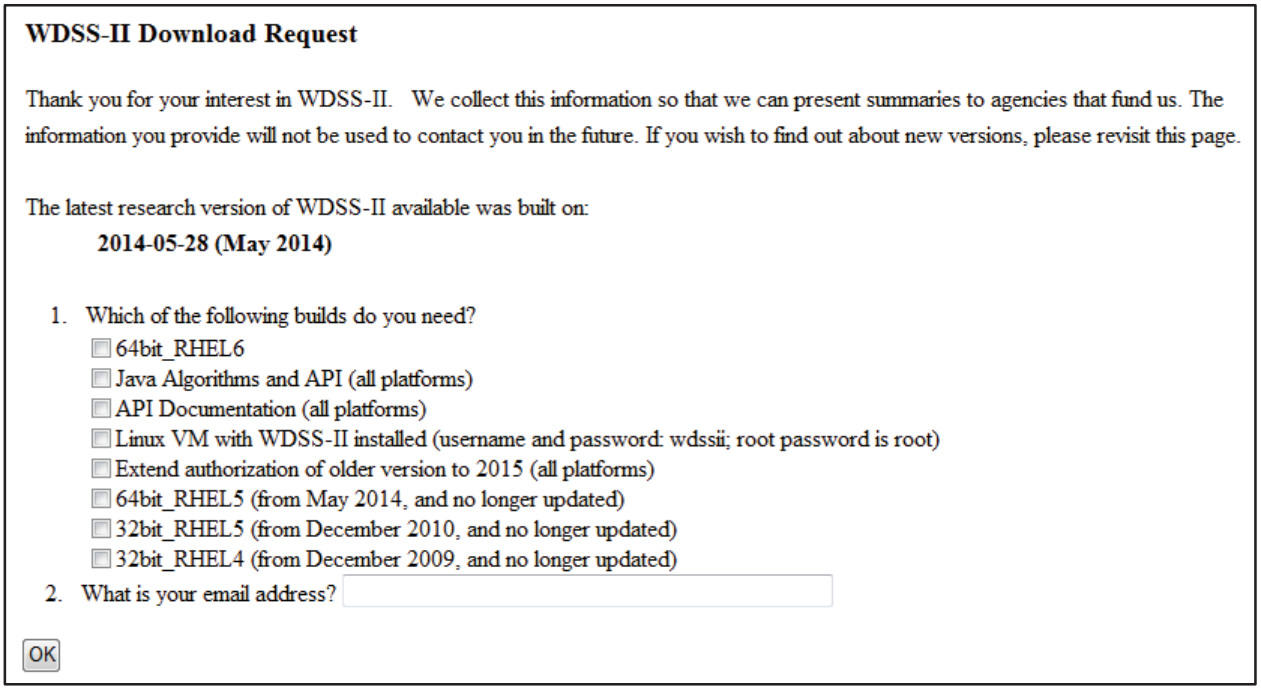
Through contacting the developers and consulting the websites of the NCAR and WDSS-II software, the AMU learned that any PC running a current Linux operating system is sufficient to run either package. The AMU has a 64-bit PC that was configured for this purpose. It has dual 2.4 GHz processors, 6 GB RAM and 1 TB of hard drive space. The freely available Linux Community Enterprise Operating System (CentOS) Release 6.4 was installed on the PC. This operating system (OS) is compatible with the RedHat Linux OS.

3 WDSS-II Preparation

This section will describe how to use WDSS-II for the dual-Doppler analyses, starting with a brief overview of how to set it up. Details are in the Appendix. Installing and running the WDSS-II software requires a working knowledge of the Linux OS. Anyone who wants to use this software package should get Linux training if not already knowledgeable.

3.1 WDSS-II Setup

The AMU accessed the WDSS-II package through a form on the website www.cimms.ou.edu/~lakshman/WDSS2/download.shtml by choosing a build (Figure **2**), providing an email address and clicking on the "OK" button. Once on the page, scroll down to "WDSS-II Download Request" to find the form. Based on the PC configuration described in section 2.2.2, the AMU chose the first configuration in the list. After clicking the "OK" button, an email from CIMMS will be sent to the address given containing a link to download the requested build.



WDSS-II Download Request

Thank you for your interest in WDSS-II. We collect this information so that we can present summaries to agencies that fund us. The information you provide will not be used to contact you in the future. If you wish to find out about new versions, please revisit this page.

The latest research version of WDSS-II available was built on:

2014-05-28 (May 2014)

1. Which of the following builds do you need?
   - ☐ 64bit_RHEL6
   - ☐ Java Algorithms and API (all platforms)
   - ☐ API Documentation (all platforms)
   - ☐ Linux VM with WDSS-II installed (username and password: wdssii; root password is root)
   - ☐ Extend authorization of older version to 2015 (all platforms)
   - ☐ 64bit_RHEL5 (from May 2014, and no longer updated)
   - ☐ 32bit_RHEL5 (from December 2010, and no longer updated)
   - ☐ 32bit_RHEL4 (from December 2009, and no longer updated)
2. What is your email address?

OK

Figure 2. The form on the WDSS-II website used to get access to the software package.

Installation and quick-start instructions are provided on the WDSS-II installation webpage (www.cimms.ou.edu/~lakshman/WDSS2/installation.shtml). The AMU first set up the Linux environment variables specific to running WDSS, which can be found on the installation and quick-start website above. Next, the command **ldd wg** was executed. This displayed all the libraries needed to run WDSS-II graphics and which ones existed in the path. Only two graphics libraries were missing. Mr. Erik Magnuson, a system and software engineer with ENSCO, Inc., assisted in setting up the graphics with the appropriate drivers and libraries. After Mr. Magnuson's assistance, the AMU executed the command **wg** in a terminal window to open the WDSS-II display with success.

For setup details, go to the Download and Setup section in the Appendix.

3.2 WDSS-II Data Processing

Once the display was working, the next step was to prepare data for the display. The data used and produced by WDSS-II tools are in netCDF format. Therefore, the data from all radars must first be converted to this format before creating and displaying radar products. Fortunately, WDSS-II has tools to process WSR-88D Level-II, TDWR, and Sigmet IRIS data formats and convert them to netCDF format. A list of WDSS-II tools and details on their usage can be found on the tools webpage: www.cimms.ou.edu/~lakshman/WDSS2/algdoc.shtml.

WSR-88D Level-II files can be converted directly into netCDF format with the **ldm2netcdf** tool. The instructions to process Level-II data are on the installation webpage (section 3.1) under the heading "Creating Netcdf Products from Level-II files." The AMU processed the KMLB data according to these instructions.

Before processing the TDWR and Sigmet IRIS data, information on their locations and VCPs must be entered into specific configuration files so WDSS-II will process them correctly. The AMU added the location information for both radars in the WDSS-II configuration file "radarinfo.xml", and created new VCP files for each. The next step was to convert the data to a format that could be processed by the **ldm2netcdf** tool. The AMU used the tools **sigmetIngestor** and **tdwrLogIngest** to do this conversion for the WSR and KMCO data, respectively, then ran **ldm2netcdf** on both output data sets to create netCDF files for working with and displaying the data in WDSS-II. The AMU then used WDSS-II tools to quality control (QC) the reflectivity data and de-alias the velocity data before further processing and display. For details on the options used with the data processing commands, read the Data Processing section in the Appendix.

3.2.1 Reflectivity Data QC

The AMU QC'd the KMLB and KMCO reflectivity data using the WDSS-II tool **w2qcnn**. It uses reflectivity, velocity, and spectrum width data gate-by-gate in a neural network to determine if a return is meteorological or not (Lackshmanan et al. 2007). The AMU ran this tool using the netCDF data output from the **ldm2netcdf** tool. The WSR data were not QC'd with **w2qcnn** because that radar software has an internal routine that QC's the reflectivity data and outputs them separate files from the non-QC'd reflectivity data. For the case data in this study, very few reflectivity gates were removed during the QC processes, perhaps due to the fact that the time periods in the data sets contained mostly meteorological targets during the severe weather events. Details on the command using **w2qcnn** are in the Appendix under the Reflectivity QC subsection in the Data Display section.

3.2.2 Velocity Data De-aliasing

Doppler radars have a maximum unambiguous radial velocity called the Nyquist velocity. If the wind speeds exceed the Nyquist velocity, the direction will change from toward (away from) the radar to away from (toward) the radar, and the magnitude of the radial winds will change in increments of twice the Nyquist velocity. For example, if the Nyquist velocity is 30 ms^{-1} and the wind speed is 35 ms^{-1},

Actual velocity toward the radar: -35 ms^{-1} + 2*30 ms^{-1} = 25 ms^{-1}

Actual velocity away from the radar: 35 ms^{-1} - 2*30 ms^{-1} = -25 ms^{-1}

In this case, actual velocities toward the radar will be displayed as away from the radar and vice versa. For stronger wind cases, the sign of the value indicating winds toward or away from the radar may not change, but the magnitude will be incorrect. Also, more than one multiple of 2*Nyquist may be needed to reduce the velocity magnitude to a value with in the Nyquist velocity interval, ±30 ms^{-1} in this example.

The KMCO velocities are de-aliased within the TDWR system and output as separate files from the aliased velocities. Therefore, the AMU did not run WDSS-II de-alias tool for this data set. The KMLB and WSR velocities, however, have no such algorithm in their systems and required de-aliasing.

3.2.2.1 KMLB

The KMLB velocity data were de-aliased with an added option, -D, to the **ldm2netcdf** command. The use of this option is described further in the Appendix in the KMLB Data Processing subsection of the Data Processing section.

Examples of aliased and de-aliased KMLB velocity data are shown in Figure 3a and b, respectively. In the color legend at the top of each image the cool colors to the left of the center gray block (0 kt) represent negative velocity values toward the radar and the warm colors to the right represent positive velocities away from the radar. The Nyquist velocity of -55.7 kt towards the radar occurs in the light purple region just left of the green, and 55.7 kt away from the radar occurs in the yellow area just right of the red.

In the lower left of Figure 3a, aliased velocities are represented by the yellow and red values in the center of the area surrounded by the circle. Going from the left of this circle toward the right, velocities were toward the radar and increasing in magnitude from -50 to -55 kt represented by the colors changing from green to light purple. Continuing to move toward the right in the center of the circle, the values abruptly changed to 53 kt away from the radar in the yellow and 40 kt away from the radar in the red. If real, this would be an area of very strong convergence, but it is more likely indicative of a level with winds stronger than -55.7 kt toward the radar. Similar aliasing is in the area surrounded by the ellipse in the upper right, except the actual velocities in this case were away from the radar. The speeds increased to 55.7 kt going from the red to yellow, but changed to -53 kt toward the radar where the color changed to light purple in the center of the yellow area. Velocity aliasing is evident in other areas of the display as well. These two areas were chosen for demonstration.

The results of the de-aliasing algorithm are shown in Figure 3b. In the circle, the velocities of 53 to 40 kt away from the radar in yellow and red became velocities toward the radar of -58 to -71 kt represented by light to medium purple. The aliased velocities in the ellipse changed from around -53 kt toward the radar to 58 kt away from the radar. The new de-aliased values were more consistent with the surrounding velocities in both speed and direction.

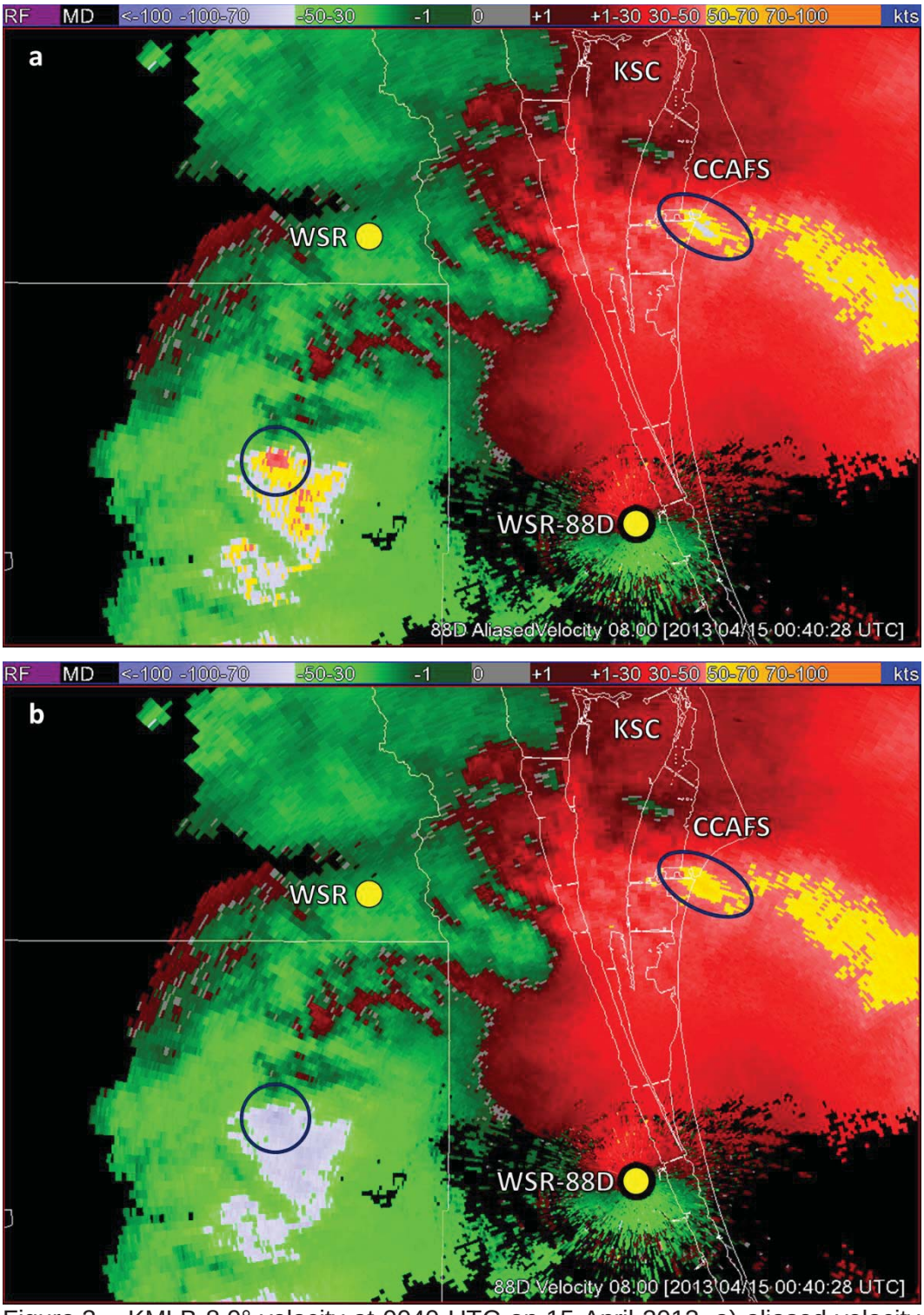


Figure 3. KMLB 8.0° velocity at 0040 UTC on 15 April 2013, a) aliased velocity and b) de-aliased velocity. The locations of the WSR-88D and 45 SW WSR radars are shown by the yellow circles, and the circle and ellipse highlight locations of the aliased (a) and de-aliased (b) velocities.

3.2.2.2 WSR

The WSR velocity data were de-aliased with the **dealias2d** tool. The use of this tool is described further in the Appendix Velocity De-aliasing subsection of the Data Processing section.

Before the data were QC'd, Ms. Crawford noticed more aliasing in the velocity data than for KMLB. The Nyquist velocity for the WSR is 21.3 m/s, or 41.4 kt. This can be seen clearly in Figure 4a. The legend at the top of the image has the same colors and values in kt as in Figure 3. The Nyquist velocity of -41.4 kt towards the radar occurs in the bright green region on the left, and 41.4 kt away from the radar occurs in the bright red area on the right. The circle to the left of the WSR radar in Figure 4a is in an area of velocities toward the radar, and the two to the right of the WSR are in an area of velocities away from the radar. Velocity aliasing is evident in these three circles as well as other areas in the display. In all three circles, velocities between the red/green boundary change abruptly from 40 kt toward the radar in the red to -41 kt away from the radar in the green.

The de-aliased velocities are shown in Figure 4b. The aliased velocities toward the radar in the circle to the left of WSR were changed from the aliased ~40 kt away from the radar to a de-aliased -84 kt toward the radar (purple). The correct de-aliased values should be in the range of -40 to -50 kt toward the radar. The velocities in the circle to the upper right of WSR experienced the same issue. Where the velocities toward the radar (green) should have been changed to 40 to 45 kt away from the radar, they were actually changed to 84 to 87 kt away from the radar. In the circle below to the lower right of WSR, the velocities toward the radar should have been de-aliased to away from the radar, but were not. The AMU noted that the WDSS-II display stated the Nyquist velocity was 62.2 kt. Looking further into the netCDF files the Nyquist velocity was found to be 31.98 ms^{-1}, or 62.2 kt. It is clear when looking at the aliased velocities in Figure 4a that the Nyquist velocity should be 41.4 kt. It is not clear how it came to be defined as 62.2 kt.

It is clear that these incorrectly de-aliased velocities cannot be used to derive a dual-Doppler wind field as the result would be erroneous. Because of this issue, the AMU decided to put these data aside and work on creating a dual-Doppler analysis between the KMLB and KMCO radars.

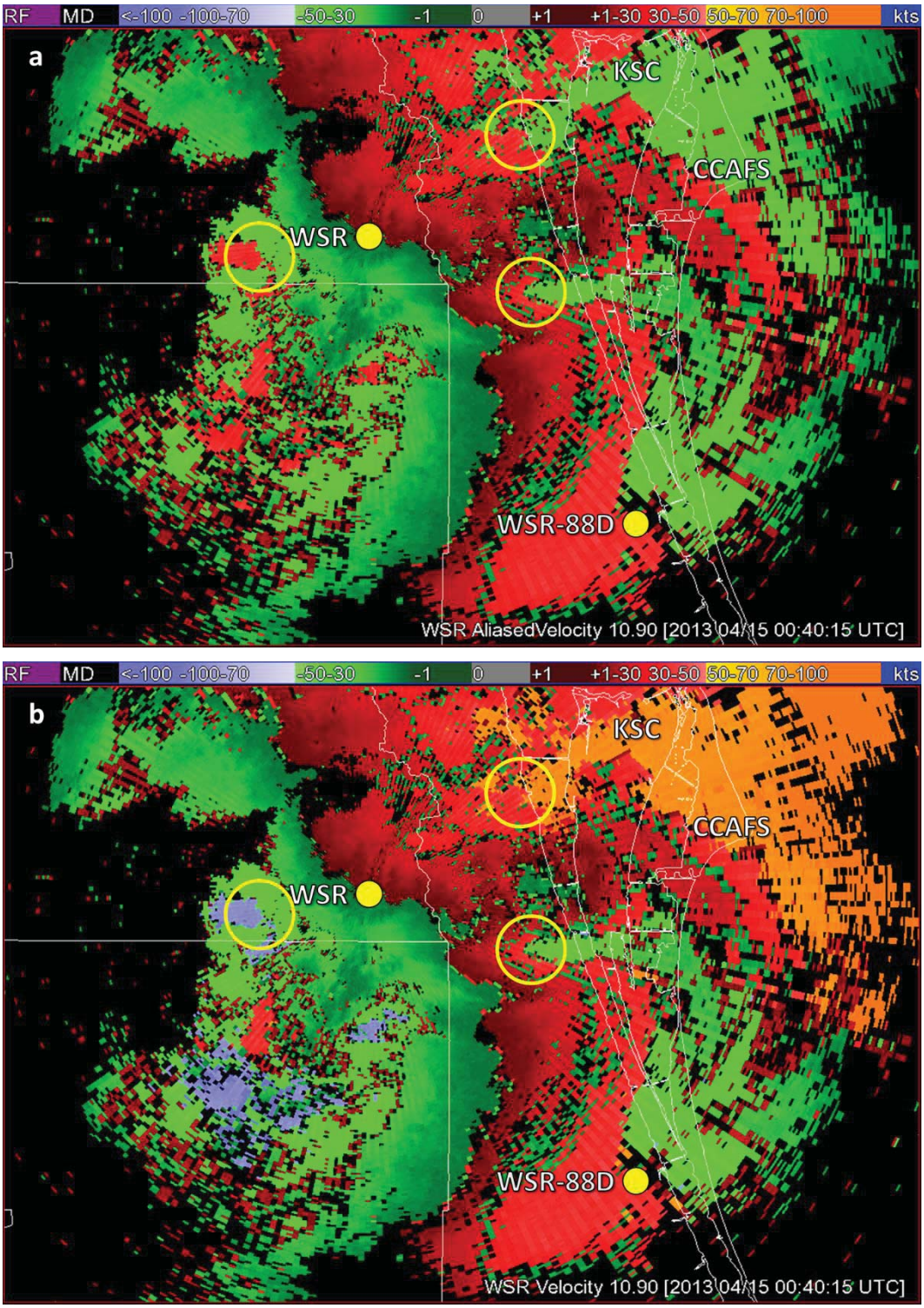


Figure 4. WSR 10.9° velocity at 0040 UTC on 15 April 2013, a) aliased velocity and b) de-aliased velocity. The locations of the WSR-88D and 45 SW WSR radars are shown by the yellow circles, and the circles highlight locations of aliased (a) and de-aliased (b) velocities.

3.3 WDSS-II Display

The first-time the AMU opened the WDSS-II graphical user interface (GUI), it had a black screen with a gray control area at the bottom (Figure 5). It is through this control area that the data are displayed. The darker gray buttons on the left in the control area are the top-level functions for the display. The first step was to load radar data. The AMU did this by clicking the **Sources** tab on the left to access the options needed to load and display the processed radar data. To add data, the AMU clicked the **Add…** button in the **Sources** tab section. This displayed the dialog box in the center of the display area in Figure 5. The AMU clicked the **Browse…** button next to the **URL** text box in the **New Source** area at the bottom of the dialog box, navigated to the directory containing the prepared 12 February KMCO data, provided the name “Feb12-KMCO” for the data set in the **Name** text box, and then clicked the **Add** button at the bottom right of the dialog box. Using the default “All” in the **History** text box loaded all the files in the directory.

After several more steps, including loading a map background, the AMU displayed the KMCO data for the severe weather event on 12 February 2014, shown in Figure 6. A tab with the name provided for the data set appeared in the **Sources** tab section containing three columns: radar products on the left, available elevation angles in the middle, and scan times on the right. For this example, the AMU chose the product ReflQC, which is QC’d reflectivity, the 0.3° elevation scan, and the initial time in the data set at 213527 UTC. Several data sets can be added through the **Sources** tab, with each having its own tab.

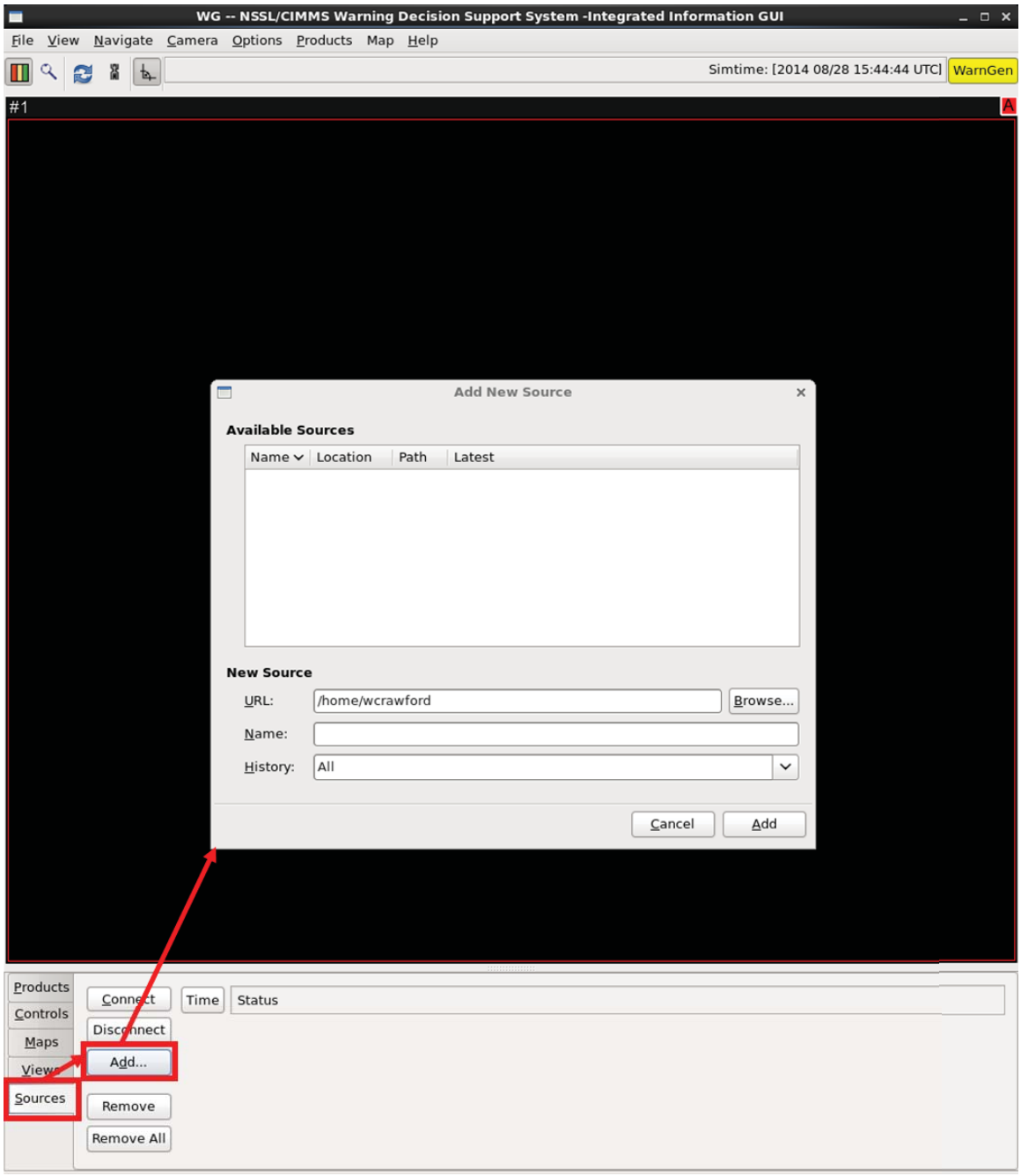


Figure 5. The initial screen in WDSS-II when issuing the **wg** command in a terminal window. The processes used to load data are highlighted by red rectangles with red arrows showing the sequence to get the dialog box that allows the user to browse for the data directory.

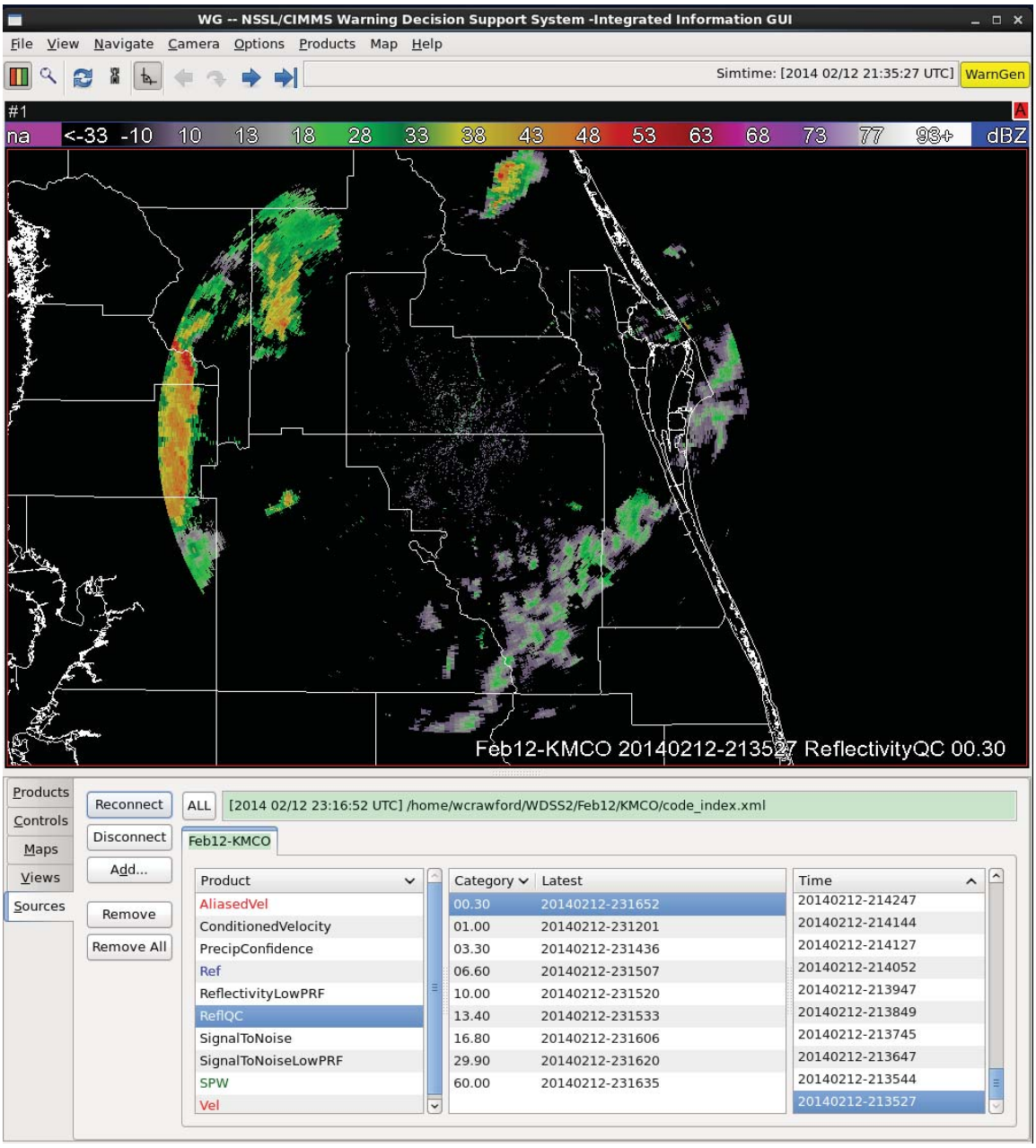


Figure 6. The WDSS-II GUI with data and map background displayed. The Sources section contains a tab named “Feb12-KMCO” with the choices of radar product (left column), elevation angle (middle column), and scan time (right column) for KMCO on 12 February 2014. The highlighted items in each list determine what is displayed: the 0.3° QC’d reflectivity at 213527 UTC.

The features in the **Products** tab, which is at the top left in the control area, allow the user to choose which radar product to display and to scroll through elevation angles and times of the displayed product. Figure 7 shows the **Products** tab contents for the same data as in Figure 6. The time, date, and elevation angle of the displayed data are shown at the top, choices to control what is displayed are under this on the left, a text box area with columns for the radar source and product is to the right of that, and controls for the elevation angle and time displayed are on the right. Multiple products can be chosen in the **Sources** tab to add in the **Products** tab text box. More details and examples are in the Data Display section of the Appendix.

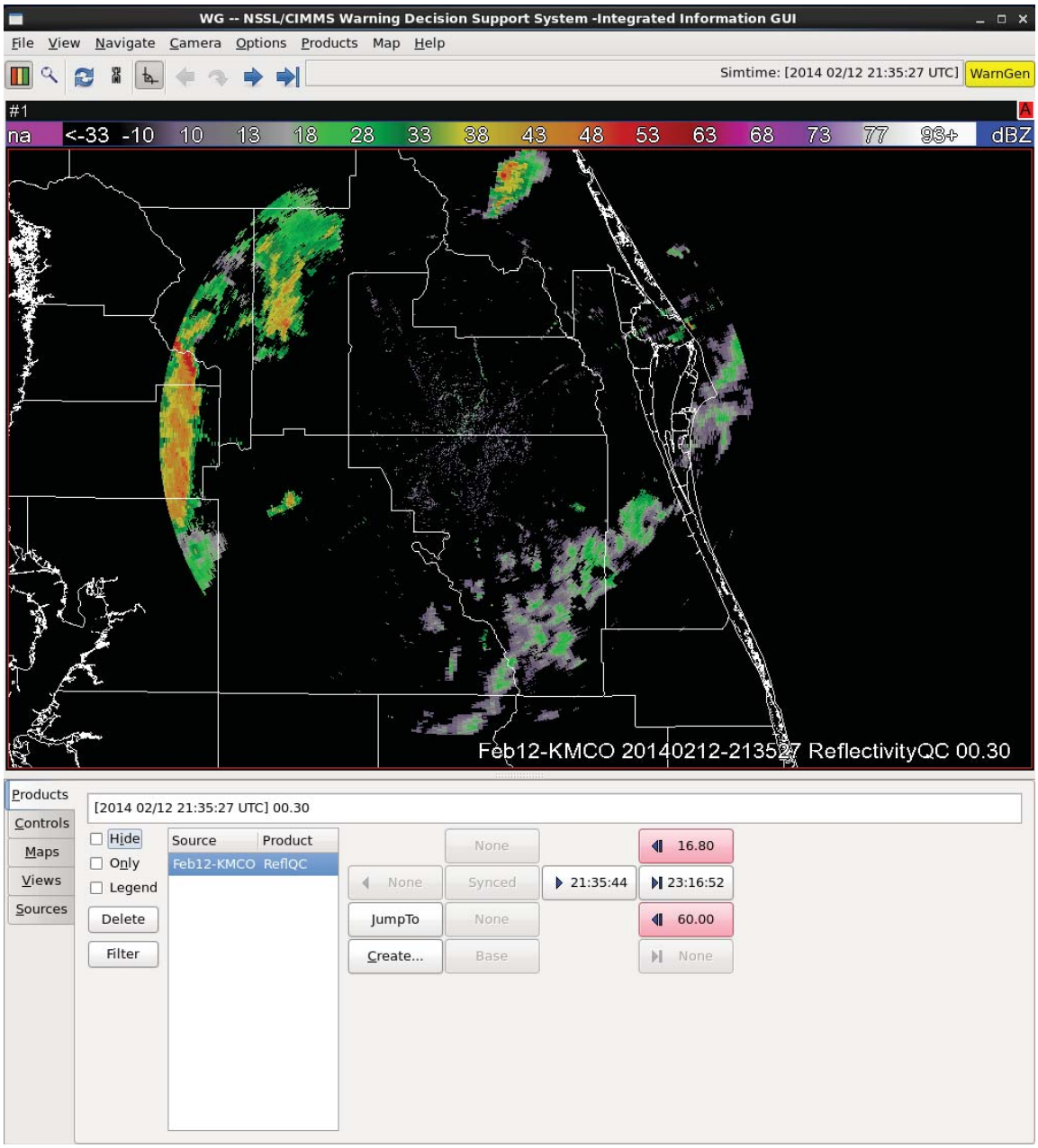


Figure 7. Same data as Figure 6, but showing the **Products** tab containing a list of the data sets that have been loaded for display and the controls for changing elevation angles and times.

4 Data Merger in WDSS-II

The goal of this task was to use data from two or more Doppler radars to create a three-dimensional (3-D) wind field over east-central Florida and the KSC/CCAFS area. Given the velocity de-aliasing issues identified with the WSR data in section 3.2.2.2, the AMU used the KMLB and KMCO data as a proof-of-concept for the analysis. The method successful in merging the KMLB and KMCO data could be used later to merge the WSR data with either of the other two radars.

The AMU researched the WDSS-II forum for how to merge data from two or more radars and found that the merging process takes several steps. First, a 3-D grid area must be created for the merge command to access. Next, a simulator tool is started that reads the processed data from two or more radars and reorders it according to time. The merger tool can then be started in another terminal window. This tool uses the output from the simulator as input, processes the data using the merging procedure described in Lakshmanan et al. (2006), and then outputs the merged data.

4.1 Merger Grid

The grid over which the merger takes place is defined by a northwest latitude/longitude (lat/lon) and grid top height, a southeast lat/lon and grid bottom height, and the horizontal and vertical grid spacing. The AMU first created the dual-Doppler lobes for KMCO and KMLB. The baseline, or distance, between the two radars is 38 NM (70.5 km), which is within the optimal range for conducting a dual-Doppler analysis as reported in Huddleston (2012). The northwest and southeast corner lat/lons of a box that encompassed both lobes, as shown in Figure 8, were used to define the merger grid corners.

The WDSS-II tool **createCache** creates the gridded area and must be run for each radar in the analysis. It computes where the data from each radar should be inserted in the 3-D grid. The output is used by the merger tool described later. Using this tool for both radars, the AMU defined a grid with a northwest corner lat/lon of 29.5 N/82 W and top of 10 km, a southeast corner lat/lon of 27 N/80 W and bottom of 0 km, and grid spacing of 0.009x0.009 degrees horizontal and 0.5 km vertical. There are approximately 111 km per degree latitude and approximately 97–99 km per degree longitude at the latitudes in the grid. The horizontal grid spacing of 0.009 is roughly equal to 1 km in both dimensions, slightly shorter in the east-west dimension than north-south. This resolution can be changed depending on operational or numerical model needs.

Details of how the AMU used the **createCache** tool are in the Data Merger Grid Setup section of the Appendix.

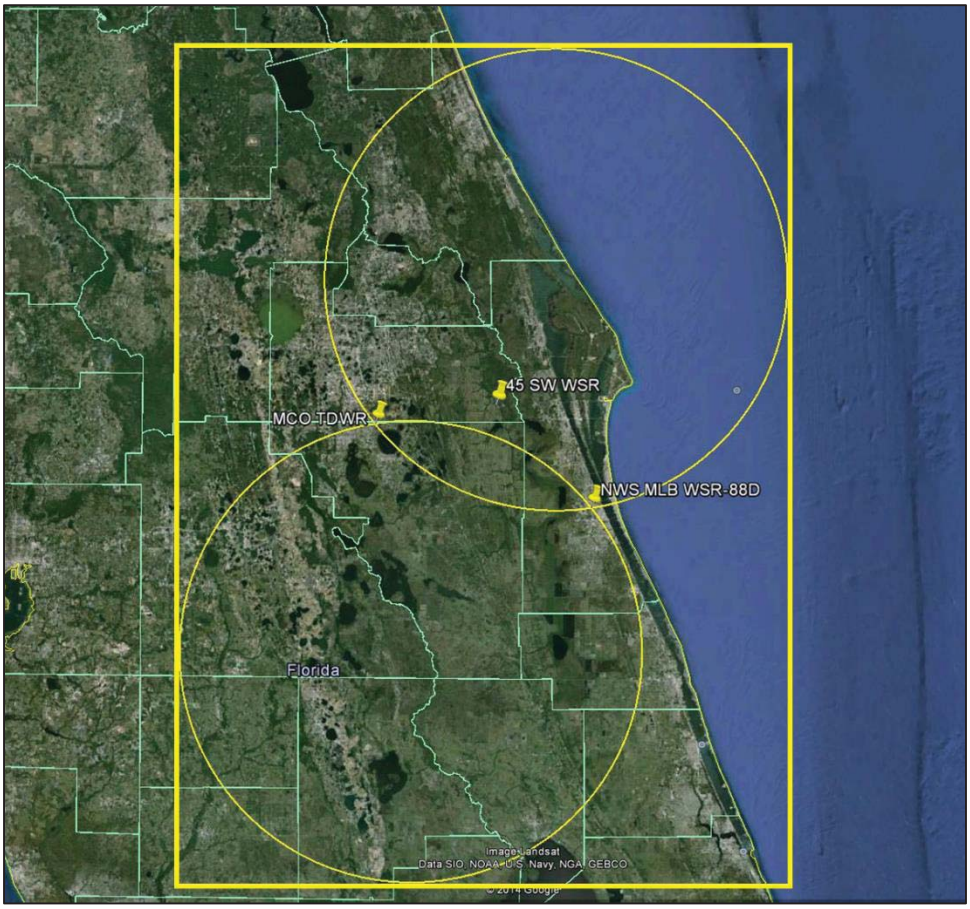


Figure 8. Google Earth image of the dual-Doppler lobes and associated merger grid outline for KMCO and KMLB.

4.2 Reflectivity Merger

According to information in the WDSS-II forum, the velocity merger requires merged reflectivity data as input. Also, the mergers must be run separately when using archived data. Therefore, the AMU created the merged reflectivity data first. Note, however, that the reflectivity and velocity mergers will be run concurrently in the real-time WDSS-II.

For mergers, two tools must be run simultaneously in separate terminal windows: **w2simulator** and **w2merger**. The first, **w2simulator**, reorders the radar scans by time and writes them out, and then **w2merger** fuses the data from the multiple radars onto the defined 3-D lat/lon grid using the procedure in Lakshmanan (2006). The inputs to **w2simulator** are the files output by **ldm2netcdf** for all radars being merged, an output directory, and the beginning and ending time for the merger, if desired. The inputs to **w2merger** are the output files from w2simulator, an output directory, and several options related to merging reflectivity. The AMU followed these procedures and was successful in merging the reflectivities between KMCO and KMLB. Details on the inputs to the tools used by the AMU are in the Reflectivity Data Merger section of the Appendix.

Figure 9 shows the reflectivity from the KMCO 0.3 degree elevation scan at 2316 UTC on 12 February 2014. The location of each radar is surrounded by a yellow circle. Note the small cone of silence, the black circle inside the yellow circle, at the KMCO radar. Figure 10 shows the reflectivity from the KMLB 0.5 degree elevation scan at 2318 UTC, the closest KMLB scan in

time to the KMCO scan in Figure 9. The cone of silence at the KMLB radar is larger than that of KMCO.

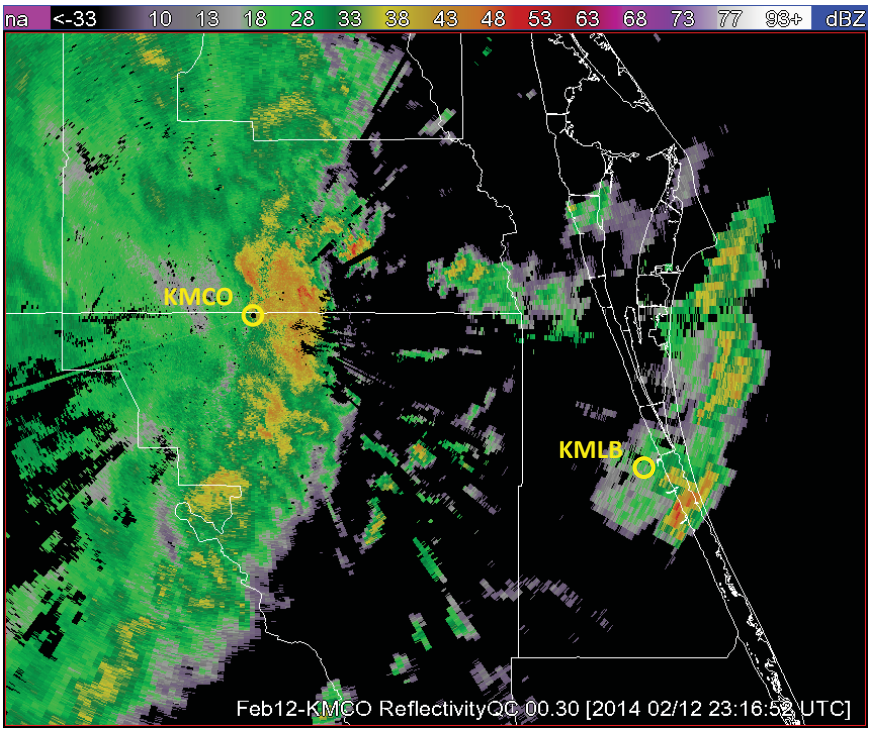


Figure 9. The KMCO reflectivity at 2316 UTC 12 February 2014, elevation angle 0.3 degrees. The yellow circles show the locations of the KMCO and KMLB radars.

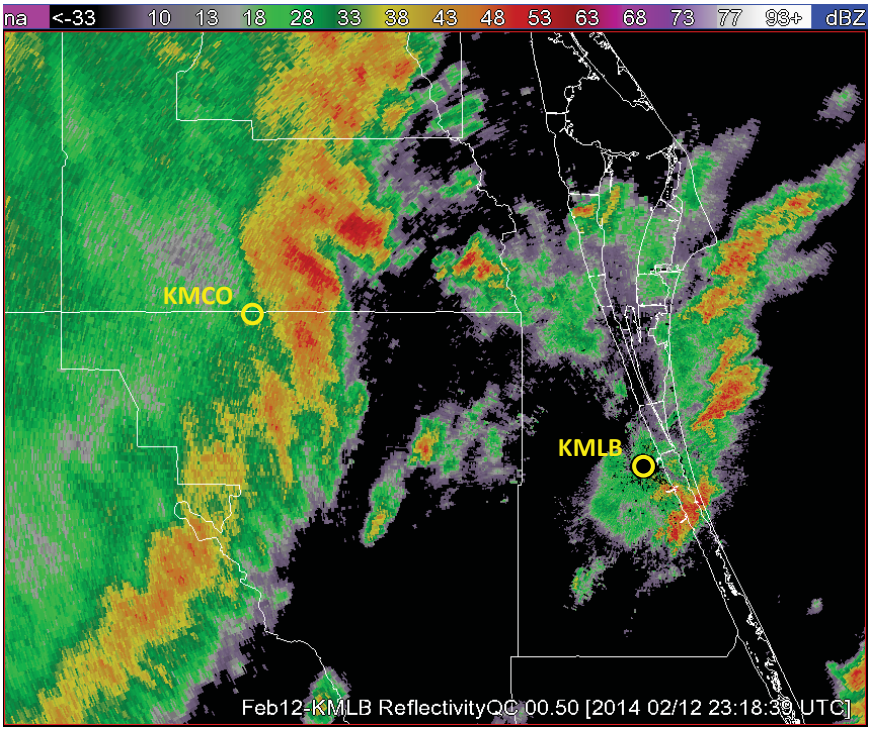


Figure 10. As in Figure 9 but for KMLB reflectivity at 2318 UTC, elevation angle 0.5 degrees.

Figure 3 shows the merged reflectivities at 2316 UTC. Note the reflectivities over the cones of silence seen in Figure 9 and Figure 10. The resolution is coarser than for either radar, KMLB has a gate spacing of 0.25 km and KMCO has a gate spacing of 0.15 km. The grid can be changed in the **createCache** tool if higher resolution is desired, but the 1-km grid spacing may be more appropriate for the merged wind field, which is the ultimate goal of this task.

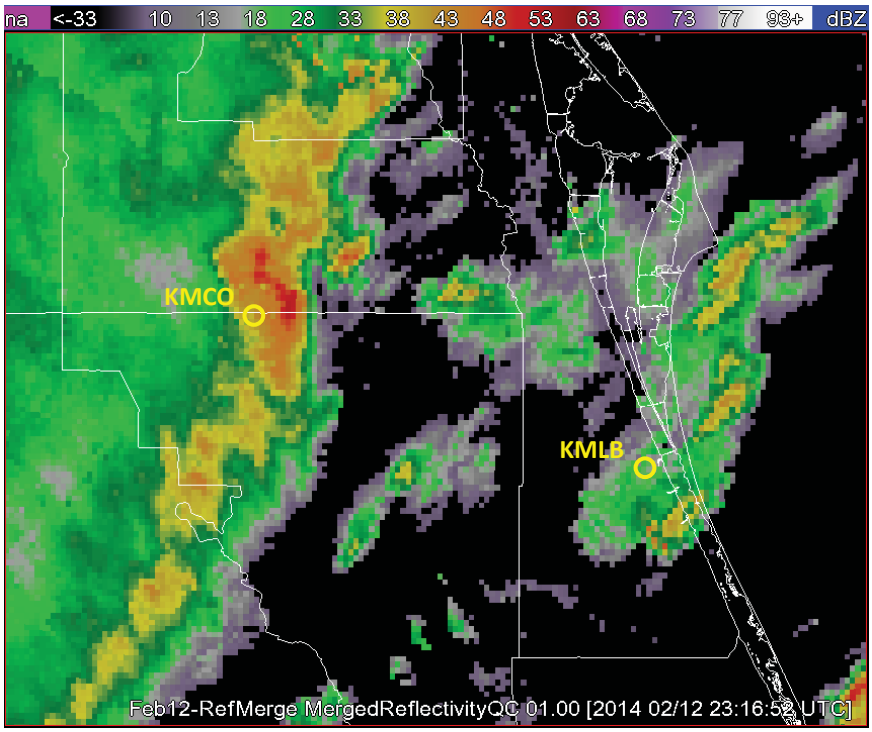


Figure 11. The KMCO and KMLB merged reflectivity at 2316 UTC 12 February 2014, height of 1 km.

4.3 Velocity Merger

The process to create merged velocities is similar to that for merged reflectivities with some differences in the inputs to the tools. The merged reflectivity must be created first as it is used as input to the velocity merger routine. The **w2simulator** tool is used to access the input data for the velocity merger, but it has the merged reflectivity as additional input. As with the reflectivities, the AMU started **w2simulator** first, and then started **w2merger** for the velocity merger in another terminal window.

The inputs to **w2simulator** are the same files are the same files as for the reflectivity merger with the addition of the output from **w2merger** for reflectivity, an output directory, and the beginning and ending time for the merger, if desired. The inputs to **w2merger** are the output files from w2simulator, an output directory, and several options related to merging velocity. The AMU followed these procedures and was unsuccessful in creating a merged wind field with the KMCO and KMLB velocity data as shown in Figure 6 of Lakshmanan et al. (2006). Details on the inputs to the tools used by the AMU are in the Velocity Data Merger section of the Appendix. The AMU searched the WDSS-II forum for ideas on what input to use in **w2simulator** and **w2merger**, asked questions on the forum when those ideas did not work, searched the WDSS-II website for documentation on using the merger tool for velocity, and tried several configurations of input to the tool.

Figure 12 shows the velocity from the KMCO 1.0 degree elevation scan at 2212 UTC on 12 February 2014. The radar locations are indicated by yellow circles. Figure 13 shows the velocity

from the KMLB 1.3 degree elevation scan at 2211 UTC, the closest KMLB scan in time and space to the KMCO scan in Figure 12.

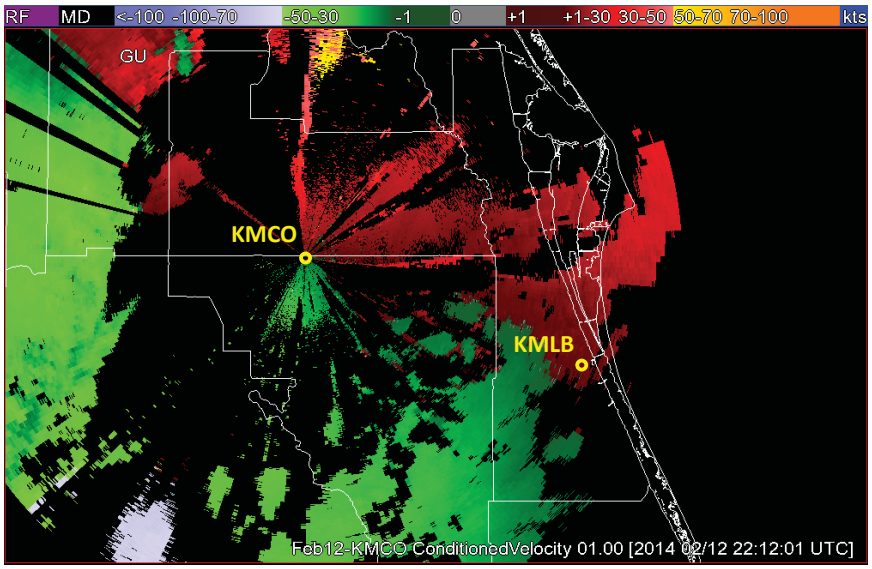


Figure 12. The KMCO velocity at 2212 UTC 12 February 2014, elevation angle 1.0 degrees. The yellow circles show the locations of the KMCO and KMLB radars.

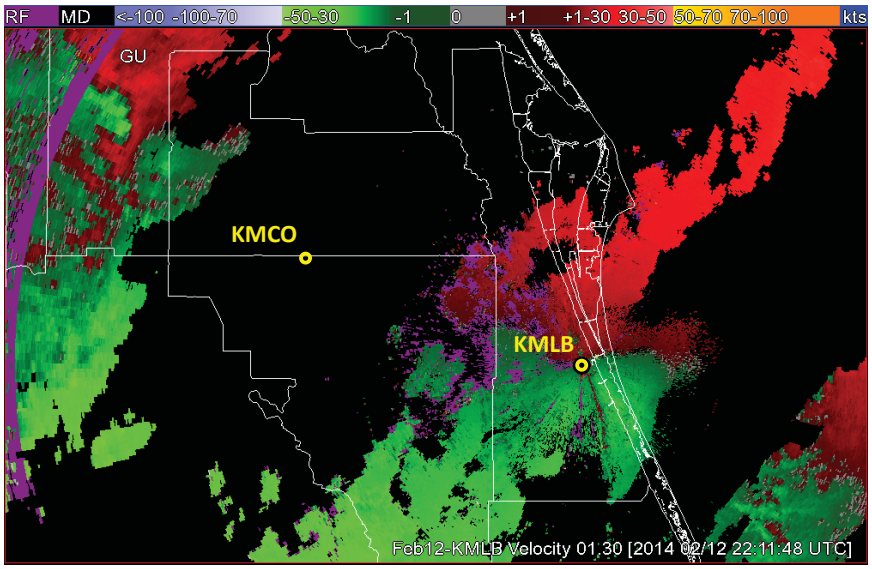


Figure 13. As in Figure 12, but for the KMLB velocity at 2211 UTC, elevation angle 1.3 degrees.

Figure 14 shows the 2211 UTC merged velocity field at 3 km. The text at the bottom of the image states that this is merged aliased velocity, but the AMU also used de-aliased velocity with the same results. The data field is uniformly purple, in the RF range of the scale at the top. The pattern of black concentric rings around KMCO is unique to this height and time, other heights and times exhibit different patterns of black rings and purple background.

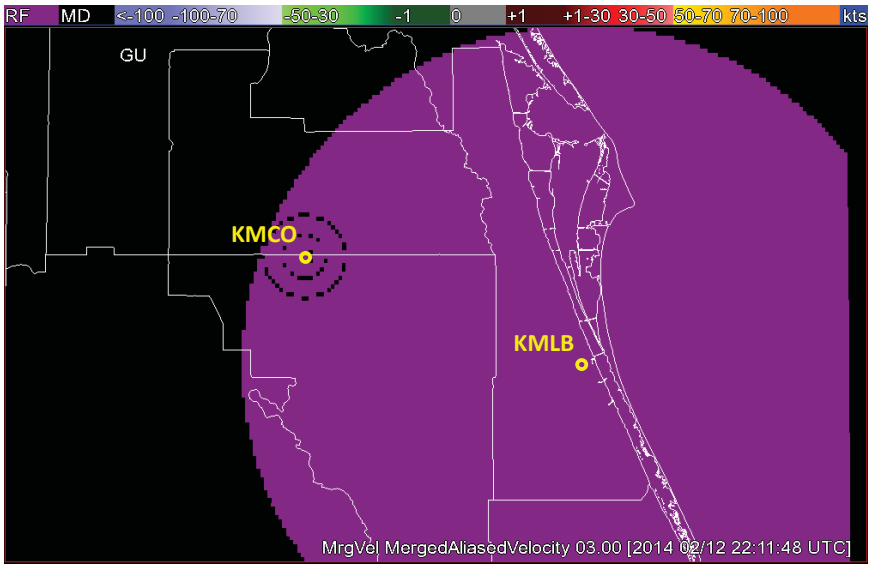


Figure 14. The KMCO and KMLB merged velocity at 2211 UTC 12 February 2014, height of 3 km.

5 Conclusions

The AMU was tasked by the 45 WS and NWS MLB to develop a dual-Doppler display using data from three local Doppler radars and freely available software to derive the wind field over east-central Florida and the KSC/CCAFS area. A display of the low-level horizontal wind field to reveal areas of high winds or convergence would be a valuable tool for forecasters in assessing the timing of high winds impacting operations, or convection initiation and subsequent lightning occurrence. This is especially important for areas where no weather observation platforms exist. The wind fields would also be used to initialize a local mesoscale numerical weather prediction model to help improve the model forecast winds, convection initiation, and other phenomena important to space launch operations and public safety.

5.1 Summary

The Doppler radars include WSR, KMLB, and KMCO and the chosen software is WDSS-II. The AMU collected data from two significant weather cases: a tornadic event on 14 April 2013 and a severe wind and hail event on 12 February 2014. For the 14 April case, the data were from WSR and KMLB. For the 12 February case, the data were from KMCO and KMLB. The AMU installed WDSS-II on a Linux PC, then processed and QC'd the radar data for display and analysis using WDSS-II tools. Because of issues with de-aliasing the WSR velocity field, the AMU did not use data from this radar in this study and only analyzed the 12 February case.

Merging the data to create the dual-Doppler analysis involved several steps. The first was to define the 3-D grid over which the analysis would take place and create grid files that the merger tools could access. The merger itself required that a simulator tool be run in the background to access the data from both radars, reorder it according to time, then create output for the merger tool to access. The AMU ran the simulator and merger tools in separate terminal windows according to WDSS-II instructions, creating the merged reflectivity first as those data are needed as input for the velocity merger. For the archived data in this task, the simulator/merger tool combination had to be run separately for the reflectivity and velocity mergers. In real-time operations, one instance of the simulation tool will run in the background for both mergers, all taking place in separate terminal windows.

The AMU was successful in creating a merged reflectivity field, which was critical to the success of creating a merged velocity field. However, the AMU was unable to replicate the results in Lakshmanan (2006) for a merged velocity field with wind barbs. The AMU researched the WDSS-II forum for discussions on similar issues, asked questions on the forum, and tested different options and values in the merger tool with no success.

5.2 Using WDSS-II

Installing and running the WDSS-II software requires a working knowledge of the Linux OS. Anyone who wants to use this software package should get Linux training if not already knowledgeable. To learn how to install and run WDSS-II and run the tools, the AMU consulted resources on the WDSS-II website, http://www.cimms.ou.edu/~lakshman/WDSS2/, including

- discussion forum (http://forum.nssl.noaa.gov/viewforum.php?f=1),
- training modules (http://www.cimms.ou.edu/~lakshman/WDSS2/w2training.shtml),
- tools (http://www.cimms.ou.edu/~lakshman/WDSS2/algdoc.shtml),
- scientific articles (http://www.cimms.ou.edu/~lakshman/WDSS2/papers.shtml), and
- other links found on the WDSS-II home page in the left column (Figure 15).

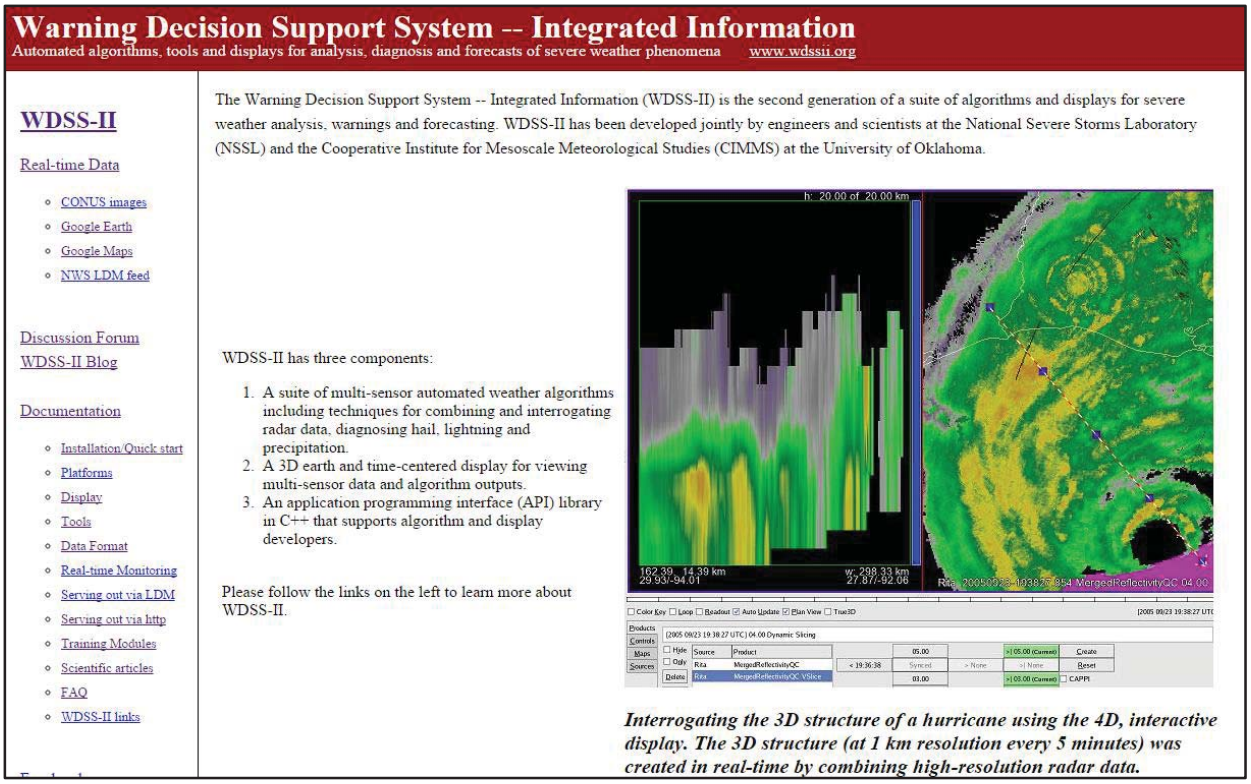


Figure 15. The top portion of the WDSS-II home page. The links with information on how to install and use WDSS-II are in the left column under the Documentation link.

The discussion forum was the most helpful of all the resources. To post questions, the AMU had to register and receive a username and password from the moderator. Searching the discussion database does not require login. The training modules were helpful, but several have out of date information and others are more focused on the network at OU. The documentation for the tools was limited. Each option is explained, but many explanations require more in-depth knowledge of the system to fully understand them. The scientific articles do not go into detail on how to use WDSS-II, but they provide good information about the science behind the system and how it can be used. The AMU did not find resources outside of the WDSS-II website with detailed explanations on how to use the system.

5.3 Recommended Future Work

Developing a dual-Doppler wind field was the main goal of this task, but that was not accomplished. It could be an issue of not using the correct options or the correct value for the options used, or there could be issues with the radar data.

The AMU is presenting the results of this task at the National Weather Association 39th Annual Meeting in October 2014. There could be other WDSS-II users present that could provide assistance in conducting this analysis. Since WDSS-II functionality favors WSR-88D radars, perhaps a merger between two of these radars could be tested to see if a velocity field can be produced. The baseline between WSR-88Ds is too large for a meaningful analysis, but if it works it would show that the issue is with the KMCO radar data. The AMU could then focus on the radar data and determine how it needs to be modified to produce a successful merged wind field. Finally, there is a follow-on AMU task to install the operational version of WDSS-II in the NWS MLB office. This will provide more opportunities to try different options and input values in order to create a merged wind field from KMCO and KMLB.

Appendix: WDSS-II Setup and Use Details

Download and Setup (Section 3.1)

The download instructions for the WDSS-II software package are in section 3.1, which is a .tgz file. Specific and easy-to-follow instructions for installing WDSS-II with this file are on the webpage www.cimms.ou.edu/~lakshman/WDSS2/installation.shtml under the title "Installation" near the top of the page. There are also instructions for setting the environment variables in the .bashrc file that exists in the home directory on a PC with a Linux OS. The final version of the .bashrc file is in Figure .

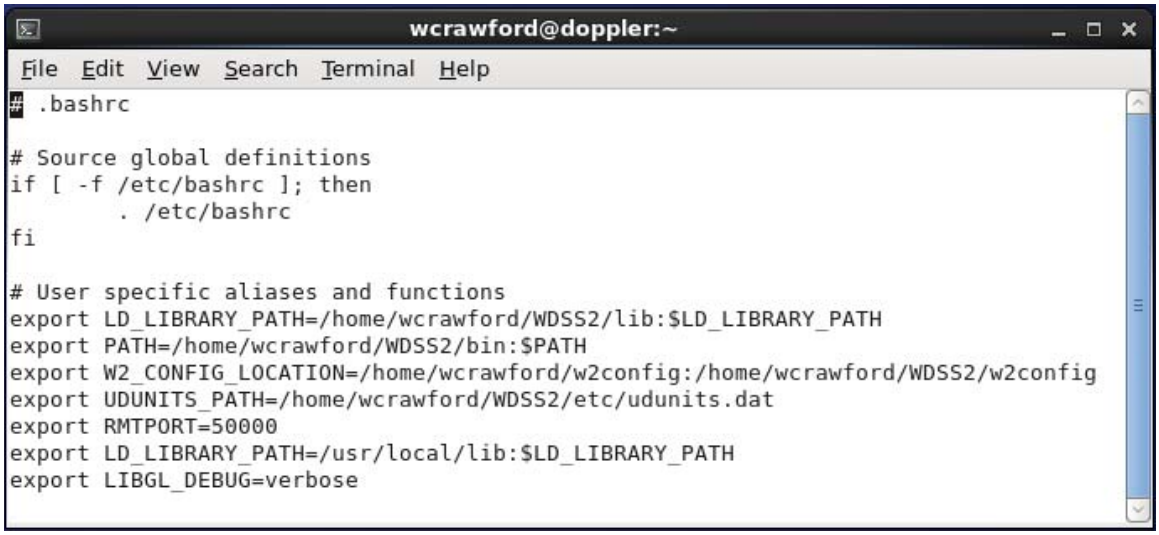


Figure 1. Content of the .bashrc file.

To get the missing graphics libraries, type "**yum** provides */libgtkglext*" to search for the appropriate library files. Once found, use "**yum** install <librarypackagename>" to install the libraries. Once installed, type "**wg**" in a terminal window to open the WDSS-II display. If there is an error, it is likely the graphics driver. For the AMU PC, Mr. Magnuson had to update the Linux kernel, disable the nouveau graphics driver, and install the Nvidia graphics driver in order for the WDSS-II display to work.

Data Processing (Section 3.2)

The data files collected from the radars needed to be processed and converted to netCDF, the format used by WDSS-II. Descriptions of the tools to do this and other analyses in WDSS-II are on the Tools webpage: www.cimms.ou.edu/~lakshman/WDSS2/algdoc.shtml.

KMLB Data Processing

The AMU converted the KMLB data directly into netCDF format using the command

ldm2netcdf -i <input directory> -o <output directory> -s KMLB -p 2014 -a -1 -D --verbose

where

- <input directory> is the full pathname of the directory containing the Level-II data,
- <output directory> is the desired directory for the output, which must exist beforehand,
- -s identifies the four-letter station name,
- -p identifies a pattern common in all filenames that need to be processed,

- -a takes no arguments and indicates the archived files will be read on startup,
- -1 takes no arguments and indicates the program will run only once since it is not operating in real time,
- -D de-aliases the velocity data, and
- --verbose outputs verbose debugging information.

This command works for WSR-88D data that have been archived at NCDC. For data collected directly from the local radar system, add the -L option to the **ldm2netcdf** command line. This option allows the command to read data files that are zipped radial-by-radial.

The de-aliasing algorithm will work more accurately if a file containing a vertical profile of the winds observed near or during the radar data period is available for **ldm2netcdf**. The user creates this file for each case using sounding or profiler data available at the time. The name of the file must be "input.snd" and must be in the same directory in which **ldm2netcdf** is executed. The first line contains the number of data levels in input.snd, the second line contains the height of the radar in feet, and the following lines contain the observations with height in feet and 1,000-ft intervals, direction in degrees, and speed in knots as in the example for the 15 April 2013 case and KMLB:

```
59
120
1000    162    20
2000    178    17
3000    184    17
6000    202    18
7000    205    17
…
61000   249    10
```

These data were from the 915- and 50-MHz profilers since no sounding was available on 15 April. In this case, there were 59 data levels with two missing at 4,000 and 5,000 ft. The program interpolates through these missing data points and outputs a file named "ewt_table" containing the wind speeds converted to ms^{-1} and separated into u and v components. The de-aliasing algorithm will use these data as a first-guess wind profile.

KMCO and WSR Location Information

The AMU had to prepare configuration files before running the algorithms to process the KMCO and WSR data files. The first step was to enter the location information for both radars in WDSS-II's radarinfo.xml file. This file can be found in the directory

/home/…/WDSS2/w2config/misc

where "…" is the user's directory. The site information for KMLB is in the original file provided with WDSS-II. At a minimum, the entries include the radar name, a user-supplied site name, latitude and longitude location, and height of the radome above sea level in meters. The AMU entered the information for the WSR in the "Military Radars" section as

```
<radar name="PAF" site="Eastern Range">
        <location lat="28.3938" lon="-80.9509" ht="47.9"/>
</radar>
```

TDWR information also requires the magnetic offset and the radar frequency. The AMU entered the information for KMCO in the "TDWR for FAA Tech Center" section as

<radar name="MCO" site="Orlando International" magnetic_offset="6W" frequency="5640">
<location lat="28.3437" lon="-81.3257" ht="51.5"/>>
</radar>

The magnetic offset changes slowly over time and should be checked and updated when needed. The AMU used the website http://magnetic-declination.com/ to get the value for Orlando. The magnetic offset option in the file does not take decimals, so the AMU rounded the value, which is currently 6.1° west.

KMCO and WSR VCP Files

Files for the WSR-88D VCPs came with the WDSS-II build, but there were none for KMCO or WSR. Therefore, the AMU created one file each for the default WSR VCP, and the two KMCO VCPs shown in Table 1. The WSR VCP file is named vcp4513 and the two KMCO VCP files are named vcp203 and vcp204 for VCP90 (Monitor) and VCP80 (Hazardous), respectively. Each file contains some header information, then a list of the elevation angles in the order they are scanned. The first element is the VCP number, the next is a logical statement of whether the radar is a WSR-88D followed by another logical statement of whether it is a clear-air VCP, the final is the time in seconds to go through a complete volume scan. The following text is the summarized content of the vcp4513 file showing the header, first and last elevation angles, and "…" representing the intermediary angles.

<vcp number="4513" isNexrad="false" isClearAir="false" totaltime="170">
<angle>0.20</angle>
…
<angle>1.80</angle>
</vcp>

The TDWR VCPs have an extra logical element, named "canCache", indicating whether a radar can change its VCP quickly. It is true for the TDWRs. The following two text groups are the summarized content of vcp203 and vcp204, respectively, showing the header, first and last elevation angles, and "…" representing the intermediary angles.

<vcp number="203" isNexrad="false" isClearAir="true" canCache="true" totaltime="360">
<angle>0.3</angle>
…
<angle>60.0</angle>
</vcp>

<vcp number="204" isNexrad="false" isClearAir="false" canCache="true" totaltime="360">
<angle>0.3</angle>
…
<angle>0.3</angle>
</vcp>

The AMU will provide these files to NWS MLB for the follow-on task.

WSR Data Processing

The AMU processed the WSR data using the command

sigmetIngestor -i <input directory> -o <output directory -s PAF -p PAF -a -1 -b 1 -v 4513 -k

where

- <input directory> is the full pathname of the directory containing the Level-II data,
- <output directory> is the desired directory for the output, which must exist beforehand,

- -s is the four-letter station name,
- -p is a pattern common in all filenames that need to be processed,
- -a takes no arguments and indicates the existing archived files will be read on startup,
- -1 takes no arguments and indicates the program will run only once since it is not operating in real time,
- -b designates the beamwidth of 1° for the WSR,
- -v specifies the VCP number to use, and
- -k will stop the algorithm from deleting the archived files.

The data in the output directory were in the format needed for ingest into **ldm2netcdf**. The AMU then converted the sigmetIngestor output to netCDF format using the command

ldm2netcdf i <input directory> -o <output directory -s PAF -p PAF -a -1 –verbose

where the input directory is the output directory for the sigmentIngestor command, and the output directory must exist beforehand. The options are the same as in the **ldm2netcdf** command for the KMLB data except for the –D de-alias option. The reasoning for excluding -D is explained in the main text.

KMCO Data Processing

The AMU processed the KMCO data using the command

tdwrLogIngest -i <input directory> -o <output directory -s MCO -p .log

where

- <input directory> is the full pathname of the directory containing the Level-II data,
- <output directory> is the desired directory for the output, which must exist beforehand,
- -s is the radar name,
- -p is a pattern common in all filenames that need to be processed,

The data in the output directory were in the format needed for ingest into **ldm2netcdf**. The AMU then converted the tdwrLogIngest output to netCDF format using the command

ldm2netcdf i <input directory> -o <output directory -s MCO -p MCO -a -1 –verbose

where the input directory is the output directory for the tdwrLogIngest command, and the output directory must exist beforehand. The options are the same as in the **ldm2netcdf** command for the KMLB data except for the –D de-alias option. The reasoning for excluding -D is explained in the main text.

Convert ldm2netcdf Output

The **ldm2netcdf** tool produces directories for every radar parameter and a directory named “code_index.fam” that is used as input (-i) to other tools and the GUI. The WDSS-II tools assume that this directory, and all directories with the *.fam extenstion, represents real-time data and will not exit upon completion. It must be converted to an xml file that WDSS-II will recognize as archived data. To convert the code_index.fam directory to an xml file, the AMU used the tool **replaceIndex** in the following command:

replaceIndex -i <home/…/code_index.fam> -o <home/…/output code_index.xml>

where

- <home/…/code_index.fam> includes the full pathname of the directory containing the code_index.fam directory, and
- <home/…/code_index.xml> is the output xml file with the same full pathname as code_index.fam.

Reflectivity QC

The AMU ran the WDSS-II QC tool, "w2qcnn", for the KMLB and KMCO data sets. The WSR system has a routine that QC's the reflectivity data in real-time and outputs both the raw and QC'd reflectivity. The AMU used the following command to QC the reflectivity data:

w2qcnn -i <home/…/code_index.xml> -o </home/…> -u -R <gate spacing x beamwidth x range>

where

- <home/…/code_index.xml> includes the full pathname of the xml file created by **replaceIndex**,
- <home/…> is the same pathname for the directory containing the code_index.xml file,
- -u QC's the data scan by scan,
- -R for KMLB is "-R 0.25x0.5x460", and
- -R for KMCO is "-R 0.15x0.5x460".

Velocity De-aliasing

The TDWR system has a de-aliasing algorithm and transmits both the aliased and de-aliased velocities, the latter called Conditioned Velocity, so this data set did not need to be de-aliased. The AMU de-aliased the KMLB data using the -D option in **ldm2netcdf**, which is the recommended method for de-aliasing WSR-88D data in WDSS-II. The AMU also used the -D option in the **ldm2netcdf** command for the WSR data, but the values output were not correct. The WDSS-II developers recommend using the **dealias2d** tool with the data output from **ldm2netcdf** for non-WSR-88D radars. The AMU used the following input to **dealias2d**:

dealias2d -i <home/…/code_index.xml> -o <home/…>

where

- <home/…/code_index.xml> is the input file including the full pathname of the xml file created by **replaceIndex**,
- <home/…> is the output directory, which is the same directory containing the code_index.xml file, and
- the ewt_table tile created by the **ldm2netdf** command for the KMLB data is copied into the same directory from which **dealias2d** is run.

The results were similar to using the -D option in **ldm2netcdf**. A discussion of this issue with images is in section 3.2.2. Given this inability to properly de-alias the WSR data and other communication issues, the AMU did not use the WSR data in the dual-Doppler analysis.

Data Display (Section 3.3)

After processing, data from all three radars can be displayed in the WDSS-II GUI. The first step is to issue the **wg** command. Figure 5 in section 3.3 shows the initial display and describes the first few steps to load the data.

Initial Display

After clicking the **Browse...** button in the initial dialog box, a new dialog box is displayed with a list of directories on the left and a list of files and directories in the highlighted directory on the right (Figure 2). The user navigates to the directory containing the code_index.xml file of the radar data desired for display, clicks on the name of the file in the right column, and then clicks **OK** in the lower right. This closes the new dialog box and returns control to the initial dialog box (Figure 3).

The full data path of the chosen data file is displayed in the **URL** text box in the New Source section of the initial dialog box. The user provides a name for the data set in the **Name** text box. In this case, the name is Feb12-KMCO, indicating the data are from KMCO during the 12 February severe weather event (section 2.1). Using the default All in the **History** drop-down menu will load all the files in the directory. The drop-down list provides choices for the number of times to load. When all choices are made, the user clicks the **Add** button, and the **Sources** section in the control area is populated with information about the radar data, as in Figure 4.

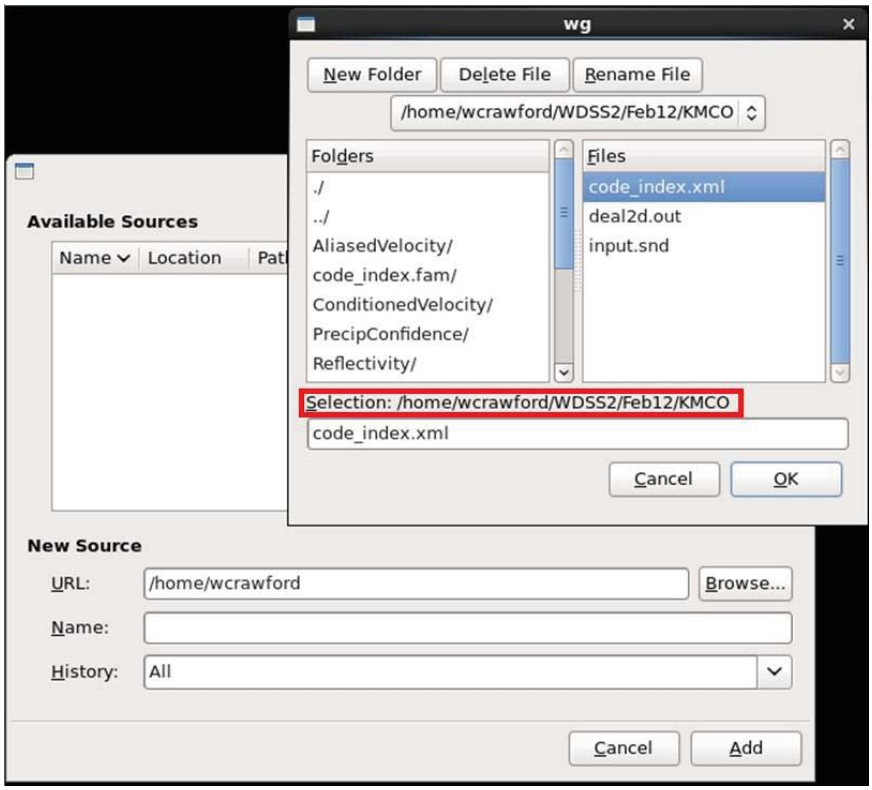


Figure 2. The new dialog box displayed after clicking the **Browse…** button on the initial dialog box (section 3.3, Figure 5). The chosen directory is surrounded by the red box, the desired code_index.xml file is highlighted in blue on the right side.

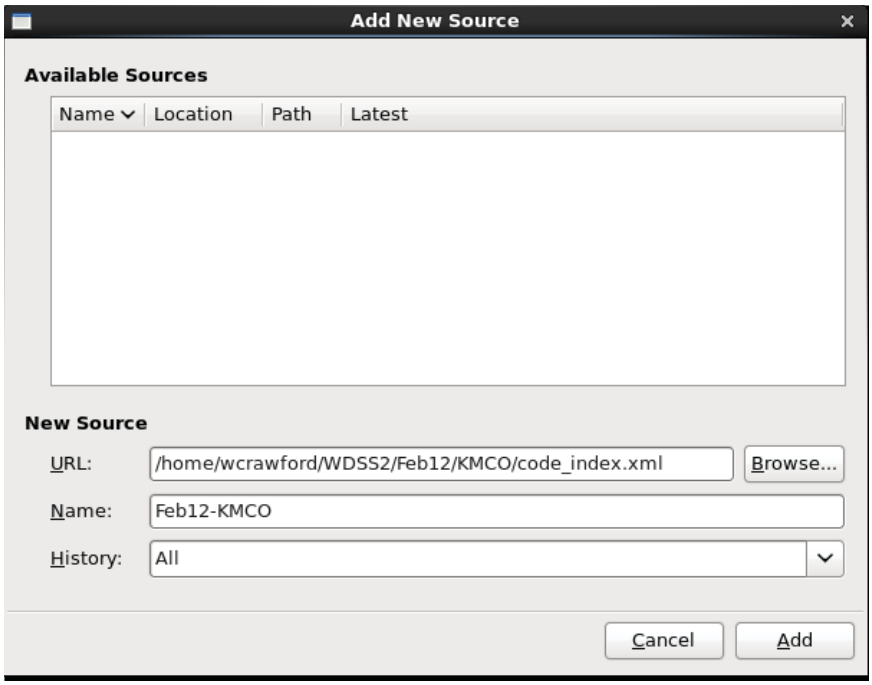


Figure 3. The initial dialog box (section 3.3, Figure 5) showing the chosen input file in the **URL** text box and the user-supplied name in the **Name** text box.

The **Sources** section in Figure 4 displays the loaded radar data parameters to choose for display (compare with section 3.3, Figure 5). The left column contains the radar products such as velocity and reflectivity, the middle column contains the available elevation angles, and the right column contains the date and time of each scan. The user chooses the parameter, elevation angle and time to display. In this example, the QC'd reflectivity from the 0.3° elevation scan at 213527 UTC is displayed.

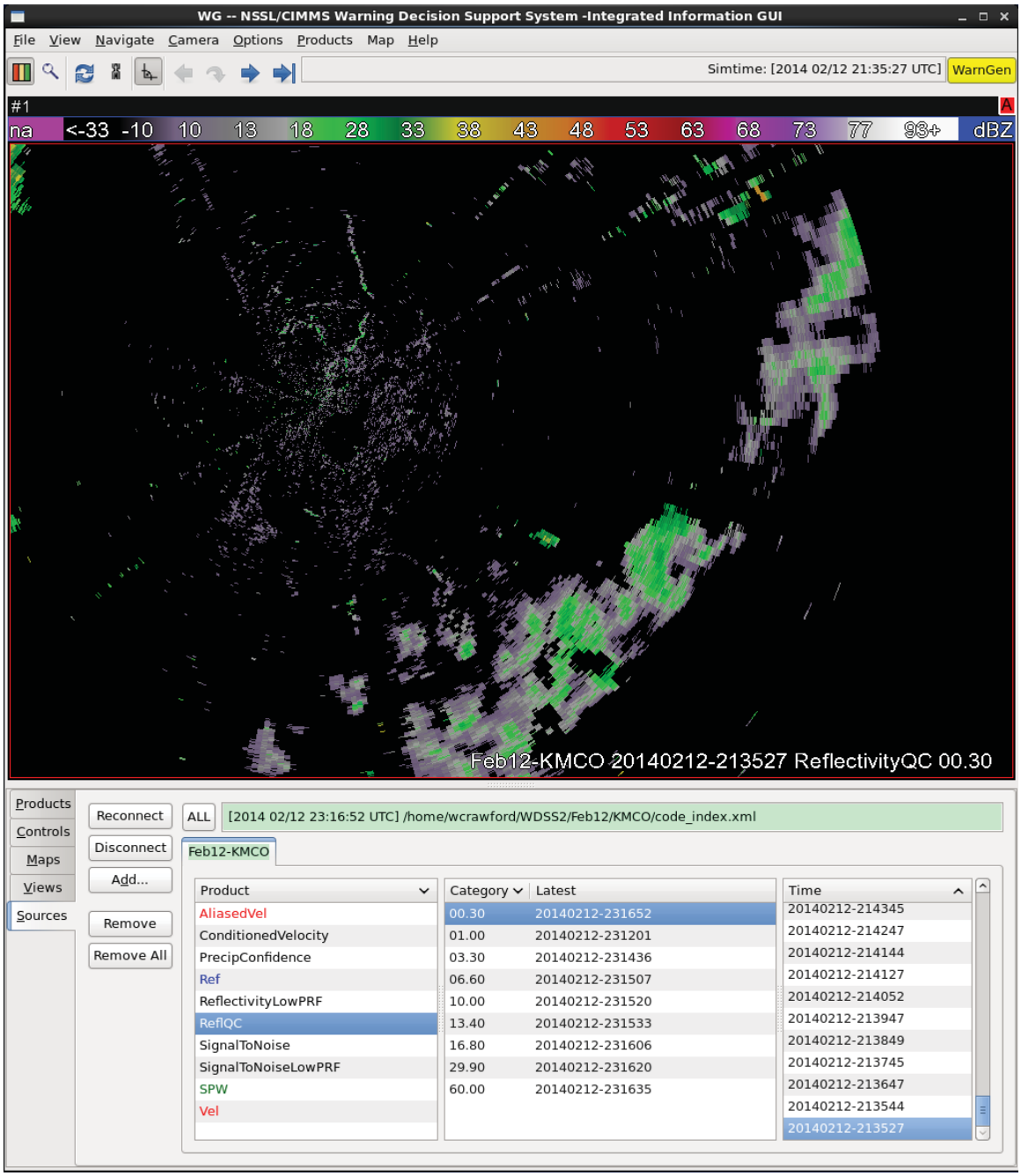


Figure 4. The WDSS-II display showing KMCO data on 12 February 2014 at 213527 UTC. The **Sources** section displays the loaded radar data parameters to choose for display. The left column contains the radar products, the middle column contains the elevation angles, and the right column contains the time of each scan.

Map Background

Figure **4** lacks a map background. In the control area at the bottom of the GUI, click the **Maps** tab to view available maps. The initial setup contains one map named Earth that is similar to an out-of-focus Google Earth map. Figure 5 shows this map overlain with the same data as in Figure 4. This is obviously not desirable. A map background showing clear state and county borders would be more useful.

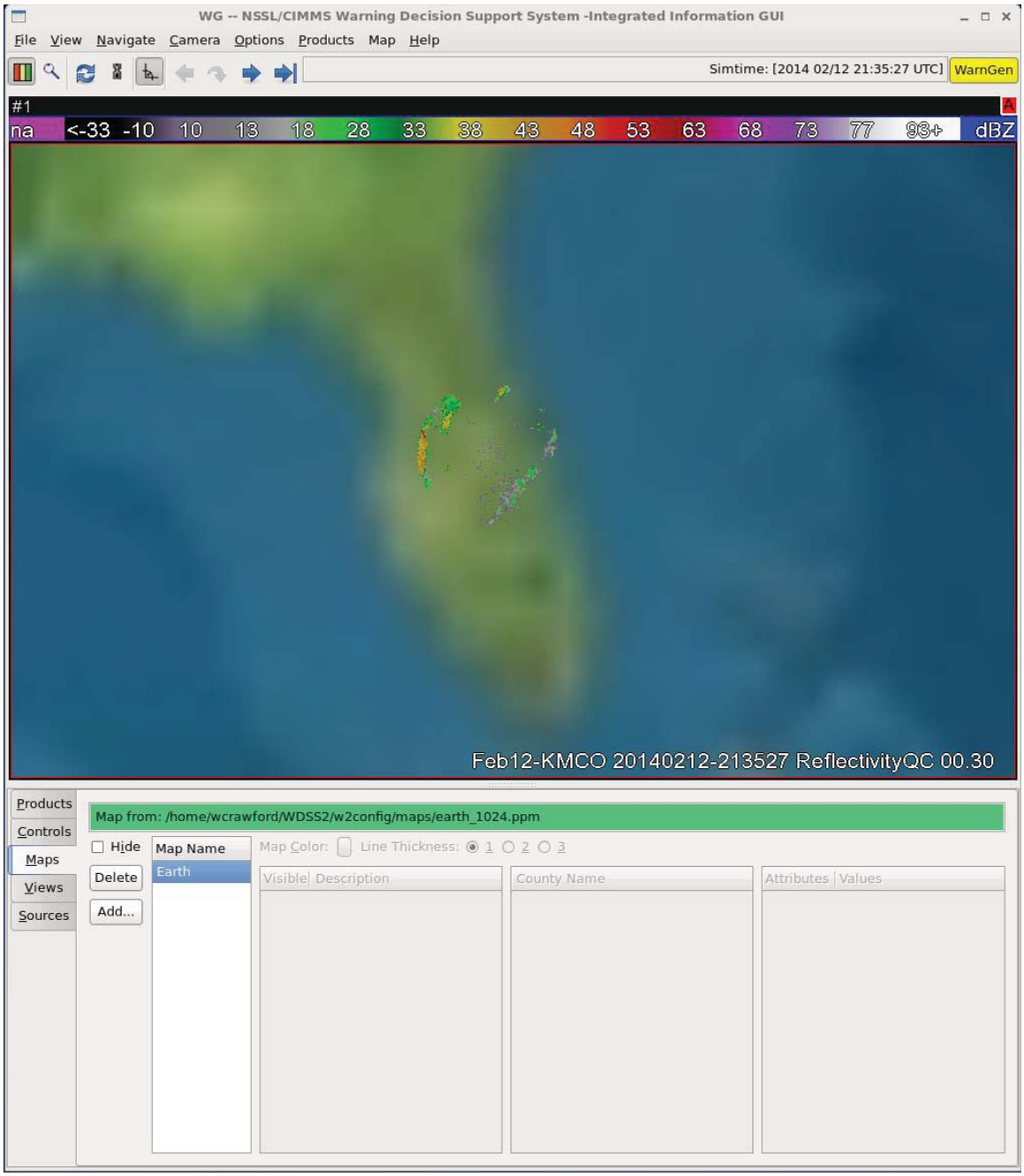


Figure 5. WDSS-II with the map background that comes with the software. The data are the same as in Figure 4, but zoomed out.

To get a map background with state and county borders, the AMU followed several steps found in the WDSS-II forum under the topic “Where to get background map shapefiles?”:

- Created a directory named **w2config** in the home directory.
- Created a directory named **shapefiles** in the new **w2config** directory.
- In the **shapefiles** directory, created a directory for each type of map named **states**, **Counties**, and **Cities**.

- On website http://www.nws.noaa.gov/geodata, downloaded the zipped files for the state, county, and city boundaries, and put them in their respective directories created in the previous step.
- Unzipped the files within each directory.
- Created a directory named **maps** in the **w2config** directory created in the first step.
- Created a file named maps.xml (Figure 6) containing information about the shapefiles needed by WDSS-II.
- Edited the .bashrc file in the home directory adding another directory path to the new w2config directory for the W2_CONFIG_LOCATION parameter. Appendix Figure 1 has this necessary addition.



Figure 6. Contents of the maps.xml file in the w2config/maps directory.

- Restarted the WDSS-II GUI and clicked on the **Maps** tab in the control area.
- Clicked on the **Add…** button and chose a map by clicking on the name in the **Add New Map** dialog box (Figure 7).
- Clicked **Add** in the lower right of the **Add New Map** dialog box. The dialog box disappears, the name of the new map file appears under **Map Name** in the **Maps** section, and the new map background is displayed (Figure 8).

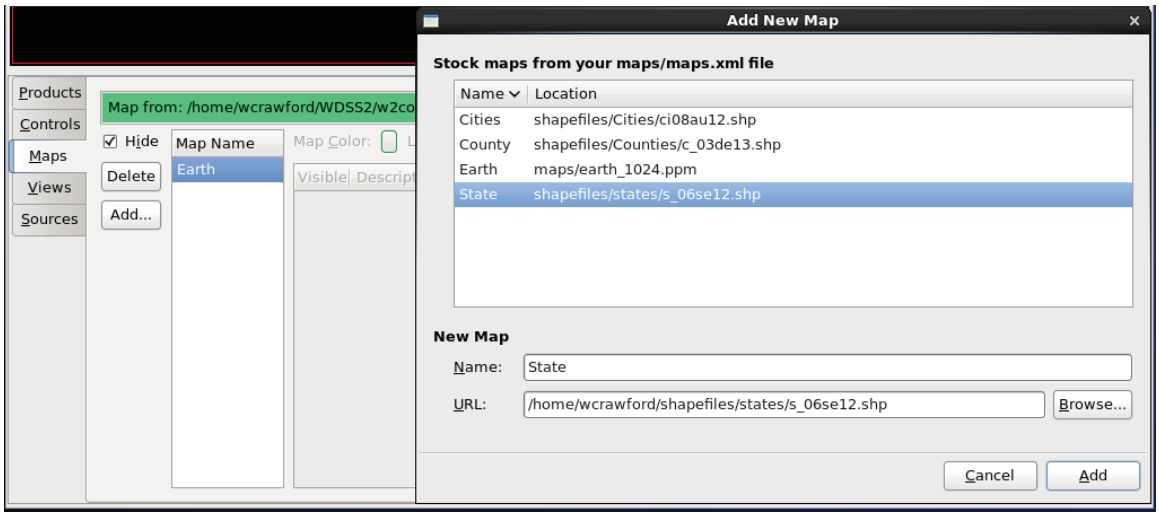


Figure 7. The **Add New Map** dialog box is displayed after clicking on **Add…** in the **Maps** menu. The State map is highlighted.

The AMU added the state map, then the county map. The cities map was too busy and created a cluttered background to the radar data. To remove the Earth map display, the AMU clicked on Earth in the **Map Name** list and checked the **Hide** box to the left of **Map Name** in the Maps tab section. This left the state and county boundaries as the map background. To delete a map, click on the map then click the **Delete** button to the left of the **Map Name** list.

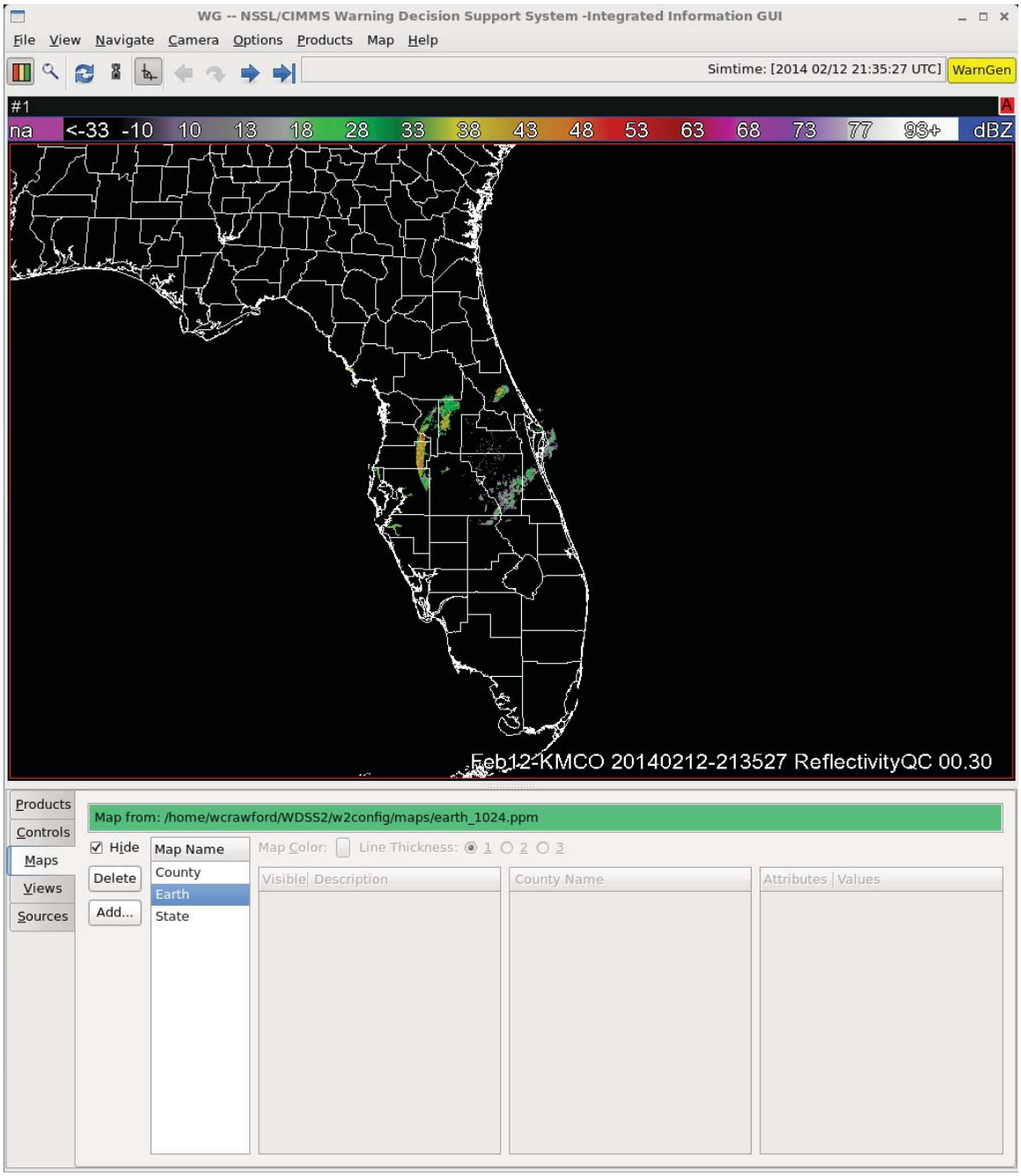


Figure 8. The WDSS-II GUI displaying the state and county boundaries using the same data and zoom level as Figure 6. The Earth map is highlighted to show how to eliminate a map background without deleting it from the list by checking the box next to **Hide** in the **Maps** section.

Choose Data to Display

Section 3.3 of the report and Appendix Figure 2, Figure 3, and Figure 4 describe how to load and display one data set, specifically the 12 February 2014 KMCO QC'd reflectivity data at 0.3° elevation. Following the same procedure described in the Initial Display section above, more than one data set can be loaded in WDSS-II through the **Sources** tab. Figure 9 shows another tab added in the Sources content for KMLB data on 12 February. The highlighted product is the

0.5° ReflQC (QC'd reflectivity) at 213306 UTC, the time closest to the KMCO data in section 3.3, Figure 6.

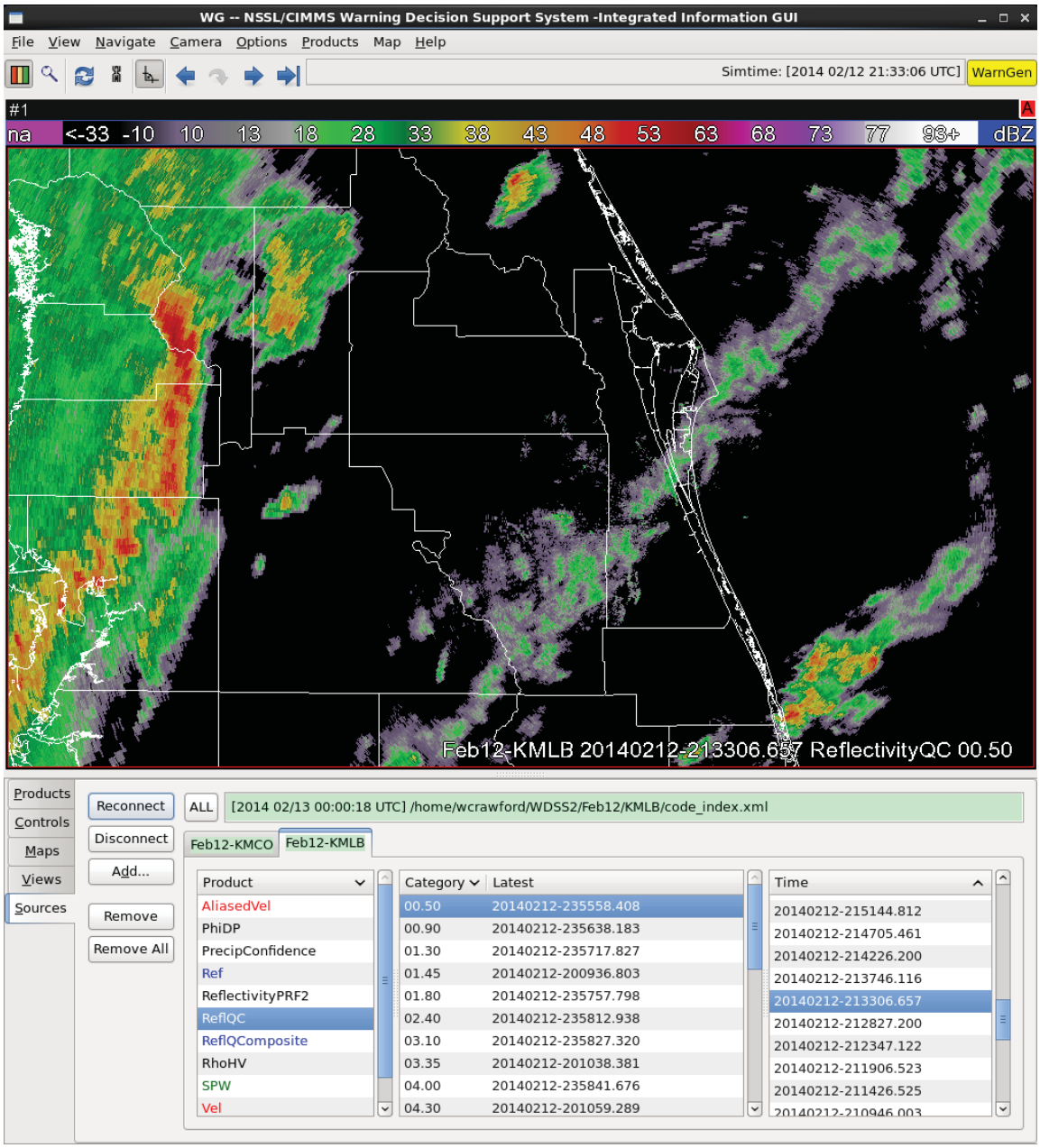


Figure 9. Similar to Figure 6 in section 3.3, except the **Sources** tab contains a second tab named "Feb12-KMLB". The highlighted items in each list determine what is displayed: the KMLB 0.5° QC'd reflectivity at 213307 UTC.

Once all three parameters of product, elevation angle, and time are chosen from one of the data source tabs in the **Sources** tab section, the data are displayed in the display area of the GUI, and the product is added to the text box in the **Products** tab section. Figure 10 shows the **Products** tab contents after choosing QC'd reflectivity and de-aliased velocity data from the 12 February KMCO and KMLB data. Information about the data is in the top text box. The choices along the left side of the **Products** tab area allows the user to hide the data, show only the selected data (no overlay with other data), display range rings and azimuth lines, delete the data set, or choose a filter for the data. The text box to the right of this area shows the products that

were chosen for display in the **Sources** tab. Note there are more than one. The area to the right of the text box controls which elevation angle and time is displayed. The forward (right) and backward (left) time buttons are outlined in red, and the upward (top) and downward (bottom) elevation angle buttons are outlined in green. The values of the next time forward or backward and of the next elevation up or down are displayed on the button. Since the lowest elevation angle of 0.5° is being displayed in Figure 10, the downward button shows the highest elevation angle of 19.5° from the previous volume scan. The buttons to the right if these display the last scan in the data set of the value shown on the button. The Display and Speed boxes below these controls allow the user to add a component of speed from a specific direction to the velocity data.

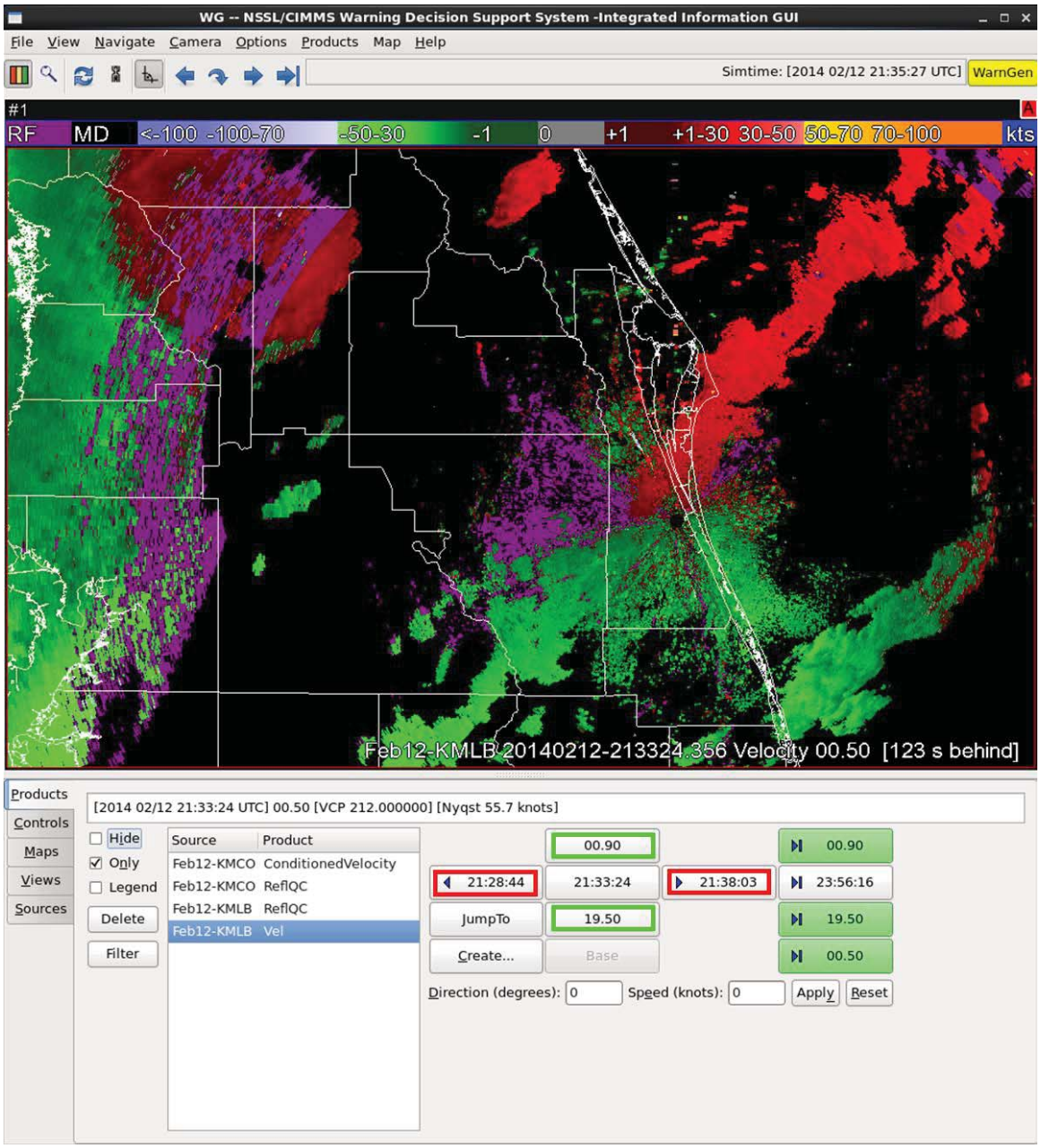


Figure 10. Similar to Figure 9, except for the de-aliased velocity at 213324 UTC and showing the **Products** tab contents. The buttons with a red box control the time displayed and the buttons with a green box control the elevation angle displayed.

Data Merger Grid Setup (Section 4.1)

The **createCache** tool must be run in the home directory. It creates a directory named .w2mergercache that contains the grid information accessed by the merger tools. The AMU used the following input to **createCache** for KMCO:

createCache -i MCO -t “29 -81.5 10” -b “27.5 -80.2 0” -s “0.009 0.009 0.5” -v “203 204” --verbose

and for KMLB:

createCache -i KMLB -t “29 -81.5 10” -b “27.5 -80.2 0” -s “0.009 0.009 0.5” –verbose

where

- -i identifies the radar name,
- -t defines the northwest corner lat/lon and top height in km of the grid,
- -b defines the southeast corner lat/lon and bottom height in km of the grid,
- -s defines the grid horizontal resolution in fractions of a degree and vertical resolution in km,
- -v defines the VCP(s) used by the radar (not needed for WSR-88D radars), and
- --verbose outputs verbose debugging information.

Reflectivity Data Merger (Section 4.2)

As stated in section 4.2, **w2simulator** must be started before **w2merger**. The AMU used the following input to **w2simulator** for the reflectivity merger:

w2simulator -i “<home/…KMCO/code_index.xml> <home/…KMLB/code_index.xml>” -o <home/…/w2sim> -c -r 1 -b 20140212-2210 -e 20140212-2300 --verbose

where

- “<home/…KMCO/code_index.xml> <home/…KMLB/code_index.xml>” includes the full pathname of the xml files created by **replaceIndex** for both radars,
- <home/…/w2sim> is the directory for the **w2simulator** output, which can be any name chosen by the user,
- -c processes only the times common to both radar data sets,
- -r indicates multiples of processing speed, where 1 equates to real-time,
- -b is the user-selected begin time of the data in the form YYYYMMDD-hhmm,
- -e is the user-selected end time of the data in the same form as –b, and
- --verbose outputs verbose debugging information.

The elements -b and -e are not required, but are helpful to use when testing algorithms. A shorter time period takes less time to process and allows evaluation of the output sooner than processing the whole data set.

Before hitting “Enter” to run the **w2simulator** tool, the AMU opened another terminal window on the Linux POC and typed the **w2merger** command line:

w2merger -i “<home/…/w2sim/index_0.fam <home/…/w2sim/index_1.fam>” -o <home/…/w2mrg> -r -t “29 -81.5 10” -b “27.5 -80.2 0” -s “0.009 0.009 0.5” -I ReflectivityQC -C 7 -3 -p 0.5 –verbose

where

- "<home/…/w2sim/index_0.fam> <home/…/w2sim/index_1.fam>" are the directories created by **w2simulator**,
- <home/…/w2mrg> is the directory for the **w2merger** output, which can be any name chosen by the user,
- -r indicates the algorithm is running in real-time even though it is an archived case,
- -t, -b, and -s are as for **createCache**,
- -I states to use the ReflectivityQC product as input (default is Reflectivity),
- -C determines the way data values are combined if they overlap in space and time where 7 is the default method,
- -3 writes a single lat/lon/height grid with all the data,
- -p is the round-off precision, and
- --verbose outputs verbose debugging information.

The AMU chose these elements for the **w2merger** command because they were recommended on the WDSS-II forum.

Once both commands were typed in separate terminal windows, the AMU executed the **w2simulator** command. As soon as the text "You can start your algorithms now" displayed in the **w2simulator** window, the AMU executed the **w2merger** command in the other terminal window.

The **w2simulator** command stopped and exited because it used .xml files as input, but the **w2merger** command did not exit since its inputs were the index_*.fam directories output by **w2simulator** (see Convert ldm2netcdf Output section above). When the **w2simulator** command had exited and the **w2merger** command had stopped, the AMU issued a Ctrl-C command in the **w2merger** window to force the command to exit.

The **w2merger** output is a code_index.fam directory that should be converted using **replaceIndex** before displaying. Once converted, follow the directions outlined in the Data Display sections above. An example of the merged reflectivity field is shown in section 4.2 Figure 11.

Velocity Data Merger (Section 4.3)

For the velocity merger, **w2simulator** must be executed again and run in conjunction with **w2merger** just as for the reflectivity merger. Before executing the commands below, run **replaceIndex** on the home/…/w2mrg/code_index.fam directory following the directions in the Convert ldm2netcdf Output subsection in the Data Processing section above. The AMU used the following input to **w2simulator** for the velocity merger:

```
w2simulator -i "<home/…KMCO/code_index.xml> <home/…KMLB/code_index.xml>
        </home/…/w2mrg/code_index.xml>" -o <home/…/w2sim> -c -r 1
        -b 20140212-2210 -e 20140212-2300 --verbose
```

where

- "<home/…KMCO/code_index.xml> <home/…KMLB/code_index.xml> </home/…/w2mrg/code_index.xml>" includes the full pathname of the xml files created by **replaceIndex** for both radars as for reflectivity and the xml file from the **w2merger** reflectivity output,

- <home/…/w2sim> is the directory for the **w2simulator** output, which can be any name chosen by the user,
- -c processes only the times common to both radar data sets,
- -r indicates multiples of processing speed, where 1 equates to real-time,
- -b is the user-selected begin time of the data in the form YYYYMMDD-hhmm,
- -e is the user-selected end time of the data in the same form as -b, and
- --verbose outputs verbose debugging information.

The elements -b and -e are not required, but are helpful to use when testing algorithms. A shorter time period takes less time to process and allows evaluation of the output sooner than processing the whole data set.

Before hitting "enter" to run the **w2simulator** tool, the AMU opened another terminal window on the Linux POC and typed the **w2merger** command line:

> w2merger -i "<home/…/w2sim/index_0.fam> <home/…/w2sim/index_1.fam> <home/…/w2sim/index_2.fam>" -o <home/…/w2mrg> -r -t "29 -81.5 10" -b "27.5 -80.2 0" -s "0.009 0.009 0.5" -I Velocity -C 8 -3 -p 0.5 -z MergedReflectivityQC:all -Z <home/…/w2mrg/code_index.xml> --verbose

where

- "<home/…/w2sim/index_0.fam <home/…/w2sim/index_1.fam> </home/…/w2sim/index_2.fam> " are the directories created by **w2simulator**,
- <home/…/w2mrg> is the directory for the **w2merger** output, which is the same as that for the reflectivity merger,
- -r indicates the algorithm is running in real-time even though it is an archived case,
- -t, -b, and -s are as for **createCache**,
- -I states to use the Velocity product as input (default is Reflectivity),
- -C determines the way data values are combined if they overlap in space and time where 8 is the method for velocity mergers,
- -3 writes a single lat/lon/height grid with all the data,
- -p is the round-off precision,
- -z identifies the reflectivity data type,
- -Z is xml file containing the merged reflectivity, and
- --verbose outputs verbose debugging information.

The AMU chose these elements for the **w2merger** command because they were recommended on the WDSS-II forum. Due to the erroneous output as shown in section 4.3, the AMU tried other options and values that produced similar results.

Once both commands were typed in separate terminal windows, the AMU executed the **w2simulator** command. As soon as the text "You can start your algorithms now" displayed in the **w2simulator** window, the AMU executed the **w2merger** command in the other terminal window.

The **w2simulator** command stopped and exited because it used .xml files as input, but the **w2merger** command did not exit since its inputs were the index_*.fam directories output by

w2simulator (see Convert ldm2netcdf Output section above). When the **w2simulator** command had exited and the **w2merger** command had stopped, the AMU issued a Ctrl-C command in the **w2merger** window to force the command to exit.

The **w2merger** output is a code_index.fam directory that should be converted using **replaceIndex** before displaying. Once converted, follow the directions outlined in the Data Display sections above.

References

Dolan, B., and S. Rutledge, 2007: An integrated display and analysis methodology for multivariable radar data. *J. Appl. Meteor. Climatol.*, **46**, 1196–1213, doi: 10.1175/JAM2524.1.

Huddleston, L., 2012: Dual-Doppler Feasibility Study. NASA Technical Memorandum TM-2012-216310, Kennedy Space Center, FL, 24 pp. [Available online at science.ksc.nasa.gov/amu/final-reports/dual-doppler-feasibility.pdf.]

Roeder, W. P., and D. A. Short, 2009: The new weather radar for America's space program: Scan Strategy Design, Preprints, *34th Conf. on Radar Meteorology*, Williamsburg, VA, Amer. Meteor. Soc., P6.2. [Available online at https://ams.confex.com/ams/pdfpapers/154174.pdf.]

Short, D., 2008: Radar Scan Strategies for the Patrick Air Force Base Weather Surveillance Radar, Model-74C, Replacement. NASA Contractor Report CR-2008-214745, Kennedy Space Center, FL, 29 pp. [Available from ENSCO, Inc., 1980 N. Atlantic Ave., Suite 830, Cocoa Beach, FL, 32931 and online at science.ksc.nasa.gov/amu/final-reports/radar-scan-strategies-radtec.pdf.]

Lakshmanan, V., A. Fritz, T. Smith, K. Hondl, and G. Stumpf, 2007: An automated technique to quality control radar reflectivity data. *J. Appl. Meteor. Climatol.*, 46, 288–305, doi: 10.1175/JAM2460.1.

Lakshmanan, V., T. Smith, K. Hondl, G. Stumpf, and A. Witt, 2006: A real-time, three-dimensional, rapidly updating, heterogeneous radar merger technique for reflectivity, velocity, and derived products. *Wea. Forecasting*, **21**, 802–823, doi:10.1175/WAF942.1.

WDSS-II links used in this task:

- Home page: http://www.cimms.ou.edu/~lakshman/WDSS2/
- Discussion forum: http://forum.nssl.noaa.gov/viewforum.php?f=1
- Training modules http://www.cimms.ou.edu/~lakshman/WDSS2/w2training.shtml
- Tools: http://www.cimms.ou.edu/~lakshman/WDSS2/algdoc.shtml
- Scientific articles: http://www.cimms.ou.edu/~lakshman/WDSS2/papers.shtml

List of Acronyms

3-D	Three Dimensional
45 SW	45th Space Wing
45 WS	45th Weather Squadron
AMU	Applied Meteorology Unit
CCAFS	Cape Canaveral Air Force Station
CentOS	Community Enterprise Operating System
CIMMS	Cooperative Institute for Mesoscale Meteorological Studies
CWA	County Warning Area
GSDO	Ground Systems Development and Operations
GUI	Graphical User Interface
IRIS	Interactive Radar Information System
KMCO	MCO TDWR
KMLB	NWS MLB WSR-88D
KSC	Kennedy Space Center
lat/lon	latitude/longitude
LSP	Launch Services Program
MCO	Orlando International Airport
NCAR	National Center for Atmospheric Research
NCDC	National Climatic Data Center
NWS MLB	National Weather Service in Melbourne, Florida
OS	Operating System
OU	University of Oklahoma
POR	Period of Record
QC	Quality Control
SLS	Space Launch System
SPG	Supplemental Product Generator
TDWR	Terminal Doppler Weather Radar
VAFB	Vandenberg Air Force Base
VCP	Volume Coverage Pattern
WDSS-II	Warning Decision Support System--Integrated Information
WSR	45 SW Weather Surveillance Radar
WSR-88D	Weather Surveillance Radar 1988 Doppler

NOTICE

Mention of a copyrighted, trademarked or proprietary product, service, or document does not constitute endorsement thereof by the author, ENSCO Inc., the AMU, the National Aeronautics and Space Administration, or the United States Government. Any such mention is solely for the purpose of fully informing the reader of the resources used to conduct the work reported herein.